

SPECTRAL STABILITY OF NONCHARACTERISTIC ISENTROPIC NAVIER–STOKES BOUNDARY LAYERS

NICOLA COSTANZINO, JEFFREY HUMPHERYS,
TOAN NGUYEN, AND KEVIN ZUMBRUN

ABSTRACT. Building on work of Barker, Humpherys, Lafitte, Rudd, and Zumbrun in the shock wave case, we study stability of compressive, or “shock-like”, boundary layers of the isentropic compressible Navier–Stokes equations with γ -law pressure by a combination of asymptotic ODE estimates and numerical Evans function computations. Our results indicate stability for $\gamma \in [1, 3]$ for all compressive boundary-layers, independent of amplitude, save for inflow layers in the characteristic limit (not treated). Expansive inflow boundary-layers have been shown to be stable for all amplitudes by Matsumura and Nishihara using energy estimates. Besides the parameter of amplitude appearing in the shock case, the boundary-layer case features an additional parameter measuring displacement of the background profile, which greatly complicates the resulting case structure. Moreover, inflow boundary layers turn out to have quite delicate stability in both large-displacement and large-amplitude limits, necessitating the additional use of a mod-two stability index studied earlier by Serre and Zumbrun in order to decide stability.

CONTENTS

1. Introduction	2
1.1. Discussion and open problems	4
2. Preliminaries	6
2.1. Lagrangian formulation.	6
2.2. Rescaled coordinates	7
2.3. Stationary boundary layers	7
2.4. Eigenvalue equations	8
2.5. Preliminary estimates	9
2.6. Evans function formulation	10
3. Main results	12
3.1. The strong layer limit	12
3.2. Analytical results	14
3.3. Numerical results	15
3.4. Conclusions	15

Date: Last Updated: June 22, 2007.

This work was supported in part by the National Science Foundation award numbers DMS-0607721 and DMS-0300487.

4. Boundary-layer analysis	16
4.1. Preliminary transformation	17
4.2. Dynamic triangularization	17
4.3. Fast/Slow dynamics	19
5. Proof of the main theorems	20
5.1. Boundary estimate	21
5.2. Convergence to D^0	23
5.3. Convergence to the shock case	24
5.4. The stability index	26
5.5. Stability in the shock limit	28
5.6. Stability for small v_0	29
6. Numerical computations	29
6.1. Winding number computations	31
6.2. Nonexistence of unstable real eigenvalues	33
6.3. The shock limit	33
6.4. Numerical convergence study	34
Appendix A. Proof of preliminary estimate: inflow case	34
Appendix B. Proof of preliminary estimate: outflow case	37
Appendix C. Nonvanishing of D_{in}^0	40
Appendix D. Nonvanishing of D_{out}^0	42
Appendix E. The characteristic limit: outflow case	44
Appendix F. Nonvanishing of D_{in} : expansive inflow case	47
References	48

1. INTRODUCTION

Consider the isentropic compressible Navier-Stokes equations

$$(1) \quad \begin{aligned} \rho_t + (\rho u)_x &= 0, \\ (\rho u)_t + (\rho u^2)_x + p(\rho)_x &= u_{xx} \end{aligned}$$

on the quarter-plane $x, t \geq 0$, where $\rho > 0$, u, p denote density, velocity, and pressure at spatial location x and time t , with γ -law pressure function

$$(2) \quad p(\rho) = a_0 \rho^\gamma, \quad a_0 > 0, \gamma \geq 1,$$

and noncharacteristic constant ‘‘inflow’’ or ‘‘outflow’’ boundary conditions

$$(3) \quad (\rho, u)(0, t) \equiv (\rho_0, u_0), \quad u_0 > 0$$

or

$$(4) \quad u(0, t) \equiv u_0 \quad u_0 < 0$$

as discussed in [25, 10, 9]. The sign of the velocity at $x = 0$ determines whether characteristics of the hyperbolic transport equation $\rho_t + u\rho_x = f$ enter the domain (considering $f := \rho u_x$ as a lower-order forcing term), and thus whether $\rho(0, t)$ should be prescribed. The variable-coefficient parabolic

equation $\rho u_t - u_{xx} = g$ requires prescription of $u(0, t)$ in either case, with $g := -\rho(u^2/2)_x - p(\rho)_x$.

By comparison, the purely hyperbolic isentropic Euler equations

$$(5) \quad \begin{aligned} \rho_t + (\rho u)_x &= 0, \\ (\rho u)_t + (\rho u^2)_x + p(\rho)_x &= 0 \end{aligned}$$

have characteristic speeds $a = u \pm \sqrt{p'(\rho)}$, hence, depending on the values of $(\rho, u)(0, t)$, may have one, two, or no characteristics entering the domain, hence require one, two, or no prescribed boundary values. In particular, there is a discrepancy between the number of prescribed boundary values for (1) and (5) in the case of mild inflow $u_0 > 0$ small (two for (1), one for (5)) or strong outflow $u_0 < 0$ large (one for (1), none for (5)), indicating the possibility of *boundary layers*, or asymptotically-constant stationary solutions of (1):

$$(6) \quad (\rho, u)(x, t) \equiv (\hat{\rho}, \hat{u})(x), \quad \lim_{z \rightarrow +\infty} (\hat{\rho}, \hat{u})(z) = (\rho_+, u_+).$$

Indeed, existence of such solutions is straightforward to verify by direct computations on the (scalar) stationary-wave ODE; see [20, 25, 19, 16, 10, 9] or Section 2.3. These may be either of “expansive” type, resembling rarefaction wave solutions on the whole line, or “compressive” type, resembling viscous shock solutions.

A fundamental question is whether or not such boundary layer solutions are *stable* in the sense of PDE. For the expansive inflow case, it has been shown in [19] that *all* boundary layers are stable, independent of amplitude, by energy estimates similar to those used to prove the corresponding result for rarefactions on the whole line. Here, we concentrate on the complementary, *compressive case* (though see discussion, Section 1.1).

Linearized and nonlinear stability of general (expansive or compressive) *small-amplitude* noncharacteristic boundary layers of (1) have been established in [19, 23, 16, 10]. More generally, it has been shown in [10, 26] that linearized and nonlinear stability are equivalent to spectral stability, or nonexistence of nonstable (nonnegative real part) eigenvalues of the linearized operator about the layer, for boundary layers of arbitrary amplitude. However, up to now the spectral stability of *large-amplitude compressive* boundary layers has remained largely undetermined.¹

We resolve this question in the present paper, carrying out a systematic, global study classifying the stability of all possible compressive boundary-layer solutions of (1). Our method of analysis is by a combination of asymptotic ODE techniques and numerical Evans function computations, following a basic approach introduced recently in [12, 3] for the study of the closely related shock wave case. Here, there are interesting complications associated with the richer class of boundary-layer solutions as compared to possible

¹ See, however, the investigations of [25] on stability index, or parity of the number of nonstable eigenvalues of the linearized operator about the layer.

shock solutions, the delicate stability properties of the inflow case, and, in the outflow case, the nonstandard eigenvalue problem arising from reduction to Lagrangian coordinates.

Our conclusions are, for both inflow and outflow conditions, that compressive boundary layers that are uniformly noncharacteristic in a sense to be made precise later (specifically, v_+ bounded away from 1, in the terminology of Section 2.3) are *unconditionally stable*, independent of amplitude, on the range $\gamma \in [1, 3]$ considered in our numerical computations. We show by energy estimates that *outflow boundary layers are stable also in the characteristic limit*. The omitted characteristic limit in the inflow case, analogous to the small-amplitude limit for the shock case should be treatable by the singular perturbation methods used in [22, 7] to treat the small-amplitude shock case; however, we do not consider this case here.

In the inflow case, our results, together with those of [19], completely resolve the question of stability of isentropic (expansive or compressive) uniformly noncharacteristic boundary layers for $\gamma \in [1, 3]$, yielding *unconditional stability independent of amplitude or type*. In the outflow case, we show stability of all compressive boundary layers without the assumption of uniform noncharacteristicity.

1.1. Discussion and open problems. The small-amplitude results obtained in [19, 16, 23, 10] are of “general type”, making little use of the specific structure of the equations. Essentially, they all require that the difference between the boundary layer solution and its constant limit at $|x| = \infty$ be small in L^1 .² As pointed out in [10], this is the “gap lemma” regime in which standard asymptotic ODE estimates show that behavior is essentially governed by the limiting constant-coefficient equations at infinity, and thus stability may be concluded immediately from stability (computable by exact solution) of the constant layer identically equal to the limiting state. These methods do not suffice to treat either the (small-amplitude) characteristic limit or the large-amplitude case, which require more refined analyses. In particular, up to now, *there was no analysis considering boundary layers approaching a full viscous shock profile, not even a profile of vanishingly small amplitude*. Our analysis of this limit indicates why: the appearance of a small eigenvalue near zero prevents uniform estimates such as would be obtained by usual types of energy estimates.

By contrast, the large-amplitude results obtained here and (for expansive layers) in [19] make use of the specific form of the equations. In particular, both analyses make use of the advantageous structure in Lagrangian coordinates. The possibility to work in Lagrangian coordinates was first pointed out by Matsumura–Nishihara [19] in the inflow case, for which the stationary boundary transforms to a moving boundary with constant speed. Here we show how to convert the outflow problem also to Lagrangian coordinates,

²Alternatively, as in [19, 23], the essentially equivalent condition that $x\hat{v}'(x)$ be small in L^1 . (For monotone profiles, $\int_0^{+\infty} |\hat{v} - v_+| dx = \pm \int_0^{+\infty} (\hat{v} - v_+) dx = \mp \int_0^{+\infty} x\hat{v}' dx$.)

by converting the resulting variable-speed boundary problem to a constant-speed one with modified boundary condition. This trick seems of general use. In particular, it might be possible that the energy methods of [19] applied in this framework would yield unconditional stability of expansive boundary-layers, completing the analysis of the outflow case. Alternatively, this case could be attacked by the methods of the present paper. These are two further interesting direction for future investigation.

In the outflow case, a further transformation to the “balanced flux form” introduced in [22], in which the equations take the form of the integrated shock equations, allows us to establish stability in the characteristic limit by energy estimates like those of [18] in the shock case. The treatment of the characteristic inflow limit by the methods of [22, 7] seems to be another extremely interesting direction for future study.

Finally, we point to the extension of the present methods to full (non-isentropic) gas dynamics and multidimensions as the two outstanding open problems in this area.

New features of the present analysis as compared to the shock case considered in [3, 12] are the presence of two parameters, strength and displacement, indexing possible boundary layers, vs. the single parameter of strength in the shock case, and the fact that the limiting equations in several asymptotic regimes possess zero eigenvalues, making the limiting stability analysis much more delicate than in the shock case. The latter is seen, for example, in the limit as a compressive boundary layer approaches a full stationary shock solution, which we show to be spectrally equivalent to the situation of unintegrated shock equations on the whole line. As the equations on the line possess always a translational eigenvalue at $\lambda = 0$, we may conclude existence of a zero at $\lambda = 0$ for the limiting equations and thus a zero *near* $\lambda = 0$ as we approach this limit, which could be stable or unstable. Similarly, the Evans function in the inflow case is shown to converge in the large-strength limit to a function with a zero at $\lambda = 0$, with the same conclusions; see Section 3 for further details.

To deal with this latter circumstance, we find it necessary to make use also of topological information provided by the stability index of [21, 8, 25], a mod-two index counting the parity of the number of unstable eigenvalues. Together with the information that there is at most one unstable zero, the parity information provided by the stability index is sufficient to determine whether an unstable zero does or does not occur. Remarkably, in the isentropic case we are able to compute explicitly the stability index for all parameter values, recovering results obtained by indirect argument in [25], and thereby completing the stability analysis in the presence of a single possibly unstable zero.

2. PRELIMINARIES

We begin by carrying out a number of preliminary steps similar to those carried out in [3, 12] for the shock case, but complicated somewhat by the need to treat the boundary and its different conditions in the inflow and outflow case.

2.1. Lagrangian formulation. The analyses of [12, 3] in the shock wave case were carried out in Lagrangian coordinates, which proved to be particularly convenient. Our first step, therefore, is to convert the Eulerian formulation (1) into Lagrangian coordinates similar to those of the shock case. However, standard Lagrangian coordinates in which the spatial variable \tilde{x} is constant on particle paths are not appropriate for the boundary-value problem with inflow/outflow. We therefore introduce instead “psuedo-Lagrangian” coordinates

$$(7) \quad \tilde{x} := \int_0^x \rho(y, t) dy, \quad \tilde{t} := t,$$

in which the physical boundary $x = 0$ remains fixed at $\tilde{x} = 0$.

Straightforward calculation reveals that in these coordinates (1) becomes

$$(8) \quad \begin{aligned} v_t - sv_{\tilde{x}} - u_{\tilde{x}} &= \sigma(t)v_{\tilde{x}} \\ u_t - su_{\tilde{x}} + p(v)_{\tilde{x}} - \left(\frac{u_{\tilde{x}}}{v}\right)_{\tilde{x}} &= \sigma(t)u_{\tilde{x}} \end{aligned}$$

on $x > 0$, where

$$(9) \quad \tilde{s} = -\frac{u_0}{v_0}, \quad \sigma(t) = m(t) - s, \quad m(t) := -\rho(0, t)u(0, t) = -u(0, t)/v(0, t),$$

so that $m(t)$ is the negative of the momentum at the boundary $x = \tilde{x} = 0$. From now on, we drop the tilde, denoting \tilde{x} simply as x .

2.1.1. Inflow case. For the inflow case, $u_0 > 0$ so we may prescribe *two* boundary conditions on (8), namely

$$(10) \quad v|_{x=0} = v_0 > 0, \quad u|_{x=0} = u_0 > 0$$

where both u_0, v_0 are constant.

2.1.2. Outflow case. For the outflow case, $u_0 < 0$ so we may prescribe *only one* boundary condition on (8), namely

$$(11) \quad u|_{x=0} = u_0 < 0.$$

Thus $v(0, t)$ is an unknown in the problem, which makes the analysis of the outflow case more subtle than that of the inflow case.

2.2. Rescaled coordinates. Our next step is to rescale the equations in such a way that coefficients remain bounded in the strong boundary-layer limit. Consider the change of variables

$$(12) \quad (x, t, v, u) \rightarrow (-\varepsilon s x, \varepsilon s^2 t, v/\varepsilon, -u/(\varepsilon s)),$$

where ε is chosen so that

$$(13) \quad 0 < v_+ < v_- = 1,$$

where v_+ is the limit as $x \rightarrow +\infty$ of the boundary layer (stationary solution) (\hat{v}, \hat{u}) under consideration and v_- is the limit as $x \rightarrow -\infty$ of its continuation into $x < 0$ as a solution of the standing-wave ODE (discussed in more detail just below). Under the rescaling (12), (8) becomes

$$(14) \quad \begin{aligned} v_t + v_x - u_x &= \sigma(t)v_x, \\ u_t + u_x + (av^{-\gamma})_x &= \sigma(t)u_x + \left(\frac{u_x}{v}\right)_x \end{aligned}$$

where $a = a_0\varepsilon^{-\gamma-1}s^{-2}$, $\sigma = -u(0, t)/v(0, t) + 1$, on respective domains

$$x > 0 \text{ (inflow case)} \quad x < 0 \text{ (outflow case)}.$$

2.3. Stationary boundary layers. Stationary boundary layers

$$(v, u)(x, t) = (\hat{v}, \hat{u})(x)$$

of (14) satisfy

$$(15) \quad \begin{aligned} (a) \quad & \hat{v}' - \hat{u}' = 0 \\ (b) \quad & \hat{u}' + (a\hat{v}^{-\gamma})' = \left(\frac{\hat{u}'}{\hat{v}}\right)' \\ (c) \quad & (\hat{v}, \hat{u})|_{x=0} = (v_0, u_0) \\ (d) \quad & \lim_{x \rightarrow \pm\infty} (\hat{v}, \hat{u}) = (v, u)_{\pm}, \end{aligned}$$

where (d) is imposed at $+\infty$ in the inflow case, $-\infty$ in the outflow case and (imposing $\sigma = 0$) $u_0 = v_0$. Using (15)(a) we can reduce this to the study of the scalar ODE,

$$(16) \quad \hat{v}' + (a\hat{v}^{-\gamma})' = \left(\frac{\hat{v}'}{\hat{v}}\right)'$$

with the same boundary conditions at $x = 0$ and $x = \pm\infty$ as above. Taking the antiderivative of this equation yields

$$(17) \quad \hat{v}' = \mathcal{H}_C(\hat{v}) = \hat{v}(\hat{v} + a\hat{v}^{-\gamma} + C),$$

where C is a constant of integration.

Noting that \mathcal{H}_C is convex, we find that there are precisely two rest points of (17) whenever boundary-layer profiles exist, except at the single parameter value on the boundary between existence and nonexistence of solutions, for which there is a degenerate rest point (double root of \mathcal{H}_C). Ignoring this degenerate case, we see that boundary layers terminating at rest point v_+ as $x \rightarrow +\infty$ must either continue backward into $x < 0$ to terminate at a

second rest point v_- as $x \rightarrow -\infty$, or else blow up to infinity as $x \rightarrow -\infty$. The first case we shall call *compressive*, the second *expansive*.

In the first case, the extended solution on the whole line may be recognized as a standing viscous shock wave; that is, *for isentropic gas dynamics, compressive boundary layers are just restrictions to the half-line $x \geq 0$ [resp. $x \leq 0$] of standing shock waves*. In the second case, as discussed in [19], the boundary layers are somewhat analogous to rarefaction waves on the whole line. From here on, we concentrate exclusively on the compressive case.

With the choice $v_- = 1$, we may carry out the integration of (16) once more, this time as a definite integral from $-\infty$ to x , to obtain

$$(18) \quad \hat{v}' = H(\hat{v}) = \hat{v}(\hat{v} - 1 + a(\hat{v}^{-\gamma} - 1)),$$

where a is found by letting $x \rightarrow +\infty$, yielding

$$(19) \quad a = -\frac{v_+ - 1}{v_+^{-\gamma} - 1} = v_+^\gamma \frac{1 - v_+}{1 - v_+^\gamma};$$

in particular, $a \sim v_+^\gamma$ in the large boundary layer limit $v_+ \rightarrow 0$. This is exactly the equation for viscous shock profiles considered in [12].

2.4. Eigenvalue equations. Linearizing (14) about (\hat{v}, \hat{u}) , we obtain

$$(20) \quad \begin{aligned} \tilde{v}_t + \tilde{v}_x - \tilde{u}_x &= \frac{\tilde{v}(0, t)}{v_0} \hat{v}' \\ \tilde{u}_t + \tilde{u}_x - \left(\frac{h(\hat{v})}{\hat{v}^{\gamma+1}} \tilde{v} \right)_x - \left(\frac{\tilde{u}_x}{\hat{v}} \right)_x &= \frac{\tilde{v}(0, t)}{v_0} \hat{u}' \\ (\tilde{v}, \tilde{u})|_{x=0} &= (\tilde{v}_0(t), 0) \\ \lim_{x \rightarrow +\infty} (\tilde{v}, \tilde{u}) &= (0, 0) \end{aligned}$$

where $v_0 = \hat{v}(0)$,

$$(21) \quad h(\hat{v}) = -\hat{v}^{\gamma+1} + a(\gamma - 1) + (a + 1)\hat{v}^\gamma$$

and \tilde{v}, \tilde{u} denote perturbations of \hat{v}, \hat{u} .

2.4.1. Inflow case. In the inflow case, $\tilde{u}(0, t) = \tilde{v}(0, t) \equiv 0$, yielding

$$(22) \quad \begin{aligned} \lambda v + v_x - u_x &= 0 \\ \lambda u + u_x - \left(\frac{h(\hat{v})}{\hat{v}^{\gamma+1}} v \right)_x &= \left(\frac{u_x}{\hat{v}} \right)_x \end{aligned}$$

on $x > 0$, with full Dirichlet conditions $(v, u)|_{x=0} = (0, 0)$.

2.4.2. Outflow case. Letting $\tilde{U} := (\tilde{v}, \tilde{u})^T$, $\hat{U} := (\hat{v}, \hat{u})^T$, and denoting by \mathcal{L} the operator associated to the linearization about boundary-layer (\hat{v}, \hat{u}) ,

$$(23) \quad \mathcal{L} := \partial_x A(x) - \partial_x B(x) \partial_x,$$

where

$$(24) \quad A(x) = \begin{pmatrix} 1 & -1 \\ -h(\hat{v})/\hat{v}^{\gamma+1} & 1 \end{pmatrix}, \quad B(x) = \begin{pmatrix} 0 & 0 \\ 0 & \hat{v}^{-1} \end{pmatrix},$$

we have $\tilde{U}_t - \mathcal{L}\tilde{U} = \frac{\tilde{v}_0(t)}{v_0}\hat{U}'(x)$, with associated eigenvalue equation

$$(25) \quad \lambda\tilde{U} - \mathcal{L}\tilde{U} = \frac{\tilde{v}(0, \lambda)}{v_0}\hat{U}'(x),$$

where $\hat{U}' = (\hat{v}', \hat{u}')$.

To eliminate the nonstandard inhomogeneous term on the righthand side of (25), we introduce a “good unknown” (c.f. [2, 6, 11, 14])

$$(26) \quad U := \tilde{U} - \lambda^{-1} \frac{\tilde{v}(0, \lambda)}{v_0} \hat{U}'(x).$$

Since $\mathcal{L}\hat{U}' = 0$ by differentiation of the boundary-layer equation, the system expressed in the good unknown becomes simply

$$(27) \quad U_t - \mathcal{L}U = 0 \quad \text{in } x < 0,$$

or, equivalently, (22) with boundary conditions

$$(28) \quad \begin{aligned} U|_{x=0} &= \frac{\tilde{v}(0, \lambda)}{v_0} (1 - \lambda^{-1}\hat{v}'(0), -\lambda^{-1}\hat{u}'(0))^T \\ \lim_{x \rightarrow +\infty} U &= 0. \end{aligned}$$

Solving for $u|_{x=0}$ in terms of $v|_{x=0}$ and recalling that $\hat{v}' = \hat{u}'$ by (18), we obtain finally

$$(29) \quad u|_{x=0} = \alpha(\lambda)v|_{x=0}, \quad \alpha(\lambda) := \frac{-\hat{v}'(0)}{\lambda - \hat{v}'(0)}.$$

Remark 2.1. *Problems (25) and (27)–(22) are evidently equivalent for all $\lambda \neq 0$, but are not equivalent for $\lambda = 0$ (for which the change of coordinates to good unknown becomes singular). For, $U = \hat{U}'$ by inspection is a solution of (27), but is not a solution of (25). That is, we have introduced by this transformation a spurious eigenvalue at $\lambda = 0$, which we shall have to account for later.*

2.5. Preliminary estimates.

Proposition 2.2 ([3]). *For each $\gamma \geq 1$, $0 < v_+ \leq 1/12 < v_0 < 1$, (18) has a unique (up to translation) monotone decreasing solution \hat{v} decaying to endstates v_{\pm} with a uniform exponential rate for v_+ uniformly bounded away from $v_- = 1$. In particular, for $0 < v_+ \leq 1/12$,*

$$(30a) \quad |\hat{v}(x) - v_+| \leq Ce^{-\frac{3(x-\delta)}{4}} \quad x \geq \delta,$$

$$(30b) \quad |\hat{v}(x) - v_-| \leq Ce^{\frac{(x-\delta)}{2}} \quad x \leq \delta$$

where δ is defined by $\hat{v}(\delta) = (v_- + v_+)/2$.

Proof. Existence and monotonicity follow trivially by the fact that (18) is a scalar first-order ODE with convex righthand side. Exponential convergence as $x \rightarrow +\infty$ follows by $H(v, v_+) = (v - v_+) \left(v - \left(\frac{1-v_+}{1-v_+^\gamma} \right) \left(\frac{1 - \left(\frac{v_+}{v} \right)^\gamma}{1 - \left(\frac{v_+}{v} \right)} \right) \right)$, whence $v - \gamma \leq \frac{H(v, v_+)}{v - v_+} \leq v - (1 - v_+)$ by $1 \leq \frac{1-x^\gamma}{1-x} \leq \gamma$ for $0 \leq x \leq 1$. Exponential convergence as $x \rightarrow -\infty$ follows by a similar, but more straightforward calculation, where, in the “centered” coordinate $\tilde{x} := x - \delta$, the constants $C > 0$ are uniform with respect to v_+, v_0 . See [3] for details. \square

The following estimates are established in Appendices A and B.

Proposition 2.3. *Nonstable eigenvalues λ of (22), i.e., eigenvalues with nonnegative real part, are confined for any $0 < v_+ \leq 1$ to the region*

$$(31) \quad \Lambda := \left\{ \lambda : \Re(\lambda) + |\Im(\lambda)| \leq \frac{1}{2} \left(2\sqrt{\gamma} + 1 \right)^2 \right\}.$$

for the inflow case, and to the region

$$(32) \quad \Lambda := \left\{ \lambda : \Re(\lambda) + |\Im(\lambda)| \leq \max \left\{ \frac{3\sqrt{2}}{2}, 3\gamma + \frac{3}{8} \right\} \right\}$$

for the outflow case.

2.6. Evans function formulation. Setting $w := \frac{u'}{\hat{v}} + \frac{h(\hat{v})}{\hat{v}^{\gamma+1}}v - u$, we may express (22) as a first-order system

$$(33) \quad W' = A(x, \lambda)W,$$

where

$$(34) \quad A(x, \lambda) = \begin{pmatrix} 0 & \lambda & \lambda \\ 0 & 0 & \lambda \\ \hat{v} & \hat{v} & f(\hat{v}) - \lambda \end{pmatrix}, \quad W = \begin{pmatrix} w \\ u - v \\ v \end{pmatrix}, \quad \prime = \frac{d}{dx},$$

where

$$(35) \quad f(\hat{v}) = \hat{v} - \hat{v}^{-\gamma}h(\hat{v}) = 2\hat{v} - a(\gamma - 1)\hat{v}^{-\gamma} - (a + 1),$$

with h as in (21) and a as in (19), or, equivalently,

$$(36) \quad f(\hat{v}) = 2\hat{v} - (\gamma - 1) \left(\frac{1 - v_+}{1 - v_+^\gamma} \right) \left(\frac{v_+}{\hat{v}} \right)^\gamma - \left(\frac{1 - v_+}{1 - v_+^\gamma} \right) v_+^\gamma - 1.$$

Remark 2.4. *The coefficient matrix A may be recognized as a rescaled version of the coefficient matrix \mathcal{A} appearing in the shock case [3, 12], with*

$$\mathcal{A} = \begin{pmatrix} 1 & 0 & 0 \\ 0 & 1 & 0 \\ 0 & 0 & \lambda \end{pmatrix} A \begin{pmatrix} 1 & 0 & 0 \\ 0 & 1 & 0 \\ 0 & 0 & 1/\lambda \end{pmatrix}.$$

The choice of variables $(w, u - v, v)^T$ may be recognized as the modified flux form of [22], adapted to the hyperbolic–parabolic case.

Eigenvalues of (22) correspond to nontrivial solutions W for which the boundary conditions $W(\pm\infty) = 0$ are satisfied. Because $A(x, \lambda)$ as a function of \hat{v} is asymptotically constant in x , the behavior near $x = \pm\infty$ of solutions of (34) is governed by the limiting constant-coefficient systems

$$(37) \quad W' = A_{\pm}(\lambda)W, \quad A_{\pm}(\lambda) := A(\pm\infty, \lambda),$$

from which we readily find on the (nonstable) domain $\Re\lambda \geq 0$, $\lambda \neq 0$ of interest that there is a one-dimensional unstable manifold $W_1^-(x)$ of solutions decaying at $x = -\infty$ and a two-dimensional stable manifold $W_2^+(x) \wedge W_3^+(x)$ of solutions decaying at $x = +\infty$, analytic in λ , with asymptotic behavior

$$(38) \quad W_j^{\pm}(x, \lambda) \sim e^{\mu_{\pm}(\lambda)x} V_j^{\pm}(\lambda)$$

as $x \rightarrow \pm\infty$, where $\mu_{\pm}(\lambda)$ and $V_j^{\pm}(\lambda)$ are eigenvalues and associated analytically chosen eigenvectors of the limiting coefficient matrices $A_{\pm}(\lambda)$. A standard choice of eigenvectors V_j^{\pm} [8, 5, 4, 13], uniquely specifying W_j^{\pm} (up to constant factor) is obtained by Kato's ODE [15], a linear, analytic ODE whose solution can be alternatively characterized by the property that there exist corresponding left eigenvectors \tilde{V}_j^{\pm} such that

$$(39) \quad (\tilde{V}_j \cdot V_j)^{\pm} \equiv \text{constant}, \quad (\tilde{V}_j \cdot \dot{V}_j)^{\pm} \equiv 0,$$

where “ \cdot ” denotes $d/d\lambda$; for further discussion, see [15, 8, 13].

2.6.1. *Inflow case.* In the inflow case, $0 \leq x \leq +\infty$, we define the *Evans function* D as the analytic function

$$(40) \quad D_{\text{in}}(\lambda) := \det(W_1^0, W_2^+, W_3^+)_{|x=0},$$

where W_j^+ are as defined above, and W_1^0 is a solution satisfying the boundary conditions $(v, u) = (0, 0)$ at $x = 0$, specifically,

$$(41) \quad W_1^0|_{x=0} = (1, 0, 0)^T.$$

With this definition, eigenvalues of \mathcal{L} correspond to zeroes of D both in location and multiplicity; moreover, the Evans function extends analytically to $\lambda = 0$, i.e., to all of $\Re\lambda \geq 0$. See [1, 8, 17, 27] for further details.

Equivalently, following [21, 3], we may express the Evans function as

$$(42) \quad D_{\text{in}}(\lambda) = (W_1^0 \cdot \widetilde{W}_1^+)_{|x=0},$$

where $\widetilde{W}_1^+(x)$ spans the one-dimensional unstable manifold of solutions decaying at $x = +\infty$ (necessarily orthogonal to the span of $W_2^+(x)$ and $W_3^+(x)$) of the adjoint eigenvalue ODE

$$(43) \quad \widetilde{W}' = -A(x, \lambda)^* \widetilde{W}.$$

The simpler representation (42) is the one that we shall use here.

2.6.2. *Outflow case.* In the outflow case, $-\infty \leq x \leq 0$, we define the *Evans function* as

$$(44) \quad D_{\text{out}}(\lambda) := \det(W_1^-, W_2^0, W_3^0)|_{x=0},$$

where W_1^- is as defined above, and W_j^0 are a basis of solutions of (33) satisfying the boundary conditions (29), specifically,

$$(45) \quad W_2^0|_{x=0} = (1, 0, 0)^T, \quad W_3^0|_{x=0} = \left(0, -\frac{\lambda}{\lambda - \hat{v}'(0)}, 1\right)^T,$$

or, equivalently, as

$$(46) \quad D_{\text{out}}(\lambda) = (W_1^- \cdot \widetilde{W}_1^0)|_{x=0},$$

where

$$(47) \quad \widetilde{W}_1^0 = \left(0, -1, -\frac{\bar{\lambda}}{\bar{\lambda} - \hat{v}'(0)}\right)^T$$

is the solution of the adjoint eigenvalue ODE dual to W_2^0 and W_3^0 .

Remark 2.5. *As discussed in Remark 2.1, D_{out} has a spurious zero at $\lambda = 0$ introduced by the coordinate change to “good unknown”.*

3. MAIN RESULTS

We can now state precisely our main results.

3.1. The strong layer limit. Taking a formal limit as $v_+ \rightarrow 0$ of the rescaled equations (14) and recalling that $a \sim v_+^\gamma$, we obtain a limiting evolution equation

$$(48) \quad \begin{aligned} v_t + v_x - u_x &= 0, \\ u_t + u_x &= \left(\frac{u_x}{v}\right)_x \end{aligned}$$

corresponding to a *pressureless gas*, or $\gamma = 0$.

The associated limiting profile equation $v' = v(v-1)$ has explicit solution

$$(49) \quad \hat{v}^0(x) = \frac{1 - \tanh\left(\frac{x-\delta}{2}\right)}{2},$$

$\hat{v}^0(0) = \frac{1 - \tanh(-\delta/2)}{2} = v_0$; the limiting eigenvalue system is $W' = A^0(x, \lambda)W$,

$$(50) \quad A^0(x, \lambda) = \begin{pmatrix} 0 & \lambda & \lambda \\ 0 & 0 & \lambda \\ \hat{v}^0 & \hat{v}^0 & f^0(\hat{v}^0) - \lambda \end{pmatrix},$$

where $f^0(\hat{v}^0) = 2\hat{v}^0 - 1 = -\tanh\left(\frac{x+\delta}{2}\right)$.

Convergence of the profile and eigenvalue equations is *uniform* on any interval $\hat{v}^0 \geq \epsilon > 0$, or, equivalently, $x - \delta \leq L$, for L any positive constant, where the sequence of coefficient matrices is therefore a *regular perturbation* of its limit. Following [12], we call $x \leq L + \delta$ the “regular region”. For $\hat{v}_0 \rightarrow 0$ on the other hand, or $x \rightarrow \infty$, the limit is less well-behaved, as may be seen

by the fact that $\partial f/\partial \hat{v} \sim \hat{v}^{-1}$ as $\hat{v} \rightarrow v_+$, a consequence of the appearance of $(\frac{v_+}{\hat{v}})$ in the expression (36) for f . Similarly, $A(x, \lambda)$ does not converge to $A_+(\lambda)$ as $x \rightarrow +\infty$ with uniform exponential rate independent of v_+ , γ , but rather as $C\hat{v}^{-1}e^{-x/2}$. As in the shock case, this makes problematic the treatment of $x \geq L + \delta$. Following [12] we call $x \geq L + \delta$ the “singular region”.

To put things in another way, the effects of pressure are not lost as $v_+ \rightarrow 0$, but rather pushed to $x = +\infty$, where they must be studied by a careful boundary-layer analysis. (Note: this is not a boundary-layer in the same sense as the background solution, nor is it a singular perturbation in the usual sense, at least as we have framed the problem here.)

Remark 3.1. *A significant difference from the shock case of [12] is the appearance of the second parameter v_0 that survives in the $v_+ \rightarrow 0$ limit.*

3.1.1. *Inflow case.* Observe that the limiting coefficient matrix

$$(51) \quad A_+^0(\lambda) := A^0(+\infty, \lambda) = \begin{pmatrix} 0 & \lambda & \lambda \\ 0 & 0 & \lambda \\ 0 & 0 & -1 - \lambda \end{pmatrix},$$

is nonhyperbolic (in ODE sense) for all λ , having eigenvalues $0, 0, -1 - \lambda$; in particular, the stable manifold drops to dimension one in the limit $v_+ \rightarrow 0$, and so the prescription of an associated Evans function is *underdetermined*.

This difficulty is resolved by a careful boundary-layer analysis in [12], determining a special “slow stable” mode

$$V_2^+ \pm (1, 0, 0)^T$$

augmenting the “fast stable” mode

$$V_3 := (\lambda/\mu)(\lambda/\mu + 1), \lambda/\mu, 1)^T$$

associated with the single stable eigenvalue $\mu = -1 - \lambda$ of A_+^0 . This determines a *limiting Evans function* $D_{\text{in}}^0(\lambda)$ by the prescription (40), (38) of Section 2.6, or alternatively via (42) as

$$(52) \quad D_{\text{in}}^0(\lambda) = (W_1^{00} \cdot \widetilde{W}_1^{0+})|_{x=0},$$

with \widetilde{W}_1^{0+} defined analogously as a solution of the adjoint limiting system lying asymptotically at $x = +\infty$ in direction

$$(53) \quad \widetilde{V}_1 := (0, -1, \bar{\lambda}/\bar{\mu})^T$$

orthogonal to the span of V_2 and V_3 , where “ $-$ ” denotes complex conjugate, and W_1^{00} defined as the solution of the limiting eigenvalue equations satisfying boundary condition (41), i.e., $(W_1^{00})|_{x=0} = (1, 0, 0)^T$.

3.1.2. *Outflow case.* We have no such difficulties in the outflow case, since $A_-^0 = A^0(-\infty)$ remains uniformly hyperbolic, and we may define a limiting Evans function D_{out}^0 directly by (44), (38), (47), at least so long as v_0 remains bounded from zero. (As perhaps already hinted by Remark 3.1, there are complications associated with the double limit $(v_0, v_+) \rightarrow (0, 0)$.)

3.2. **Analytical results.** With the above definitions, we have the following main theorems characterizing the strong-layer limit $v_+ \rightarrow 0$ as well as the limits $v_0 \rightarrow 0, 1$.

Theorem 3.2. *For $v_0 \geq \eta > 0$ and λ in any compact subset of $\Re\lambda \geq 0$, $D_{\text{in}}(\lambda)$ and $D_{\text{out}}(\lambda)$ converge uniformly to $D_{\text{in}}^0(\lambda)$ and $D_{\text{out}}^0(\lambda)$ as $v_+ \rightarrow 0$.*

Theorem 3.3. *For λ in any compact subset of $\Re\lambda \geq 0$ and v_+ bounded from 1, $D_{\text{in}}(\lambda)$, appropriately renormalized by a nonvanishing analytic factor, converges uniformly as $v_0 \rightarrow 1$ to the Evans function for the (unintegrated) eigenvalue equations of the associated viscous shock wave connecting $v_- = 1$ to v_+ ; likewise, $D_{\text{out}}^0(\lambda)$, appropriately renormalized, converges uniformly as $v_0 \rightarrow 0$ to the same limit for λ uniformly bounded away from zero.*

By similar computations, we obtain also the following direct result.

Theorem 3.4. *Inflow boundary layers are stable for v_0 sufficiently small.*

We have also the following parity information, obtained by stability-index computations as in [25].³

Lemma 3.5 (Stability index). *For any $\gamma \geq 1$, v_0 , and v_+ , $D_{\text{in}}(0) \neq 0$, hence the number of unstable roots of D_{in} is even; on the other hand $D_{\text{in}}^0(0) = 0$ and $\lim_{v_0 \rightarrow 0} D_{\text{in}}^0(\lambda) \equiv 0$. Likewise, $(D_{\text{in}}^0)'(0)$, $D_{\text{out}}'(0) \neq 0$, $(D_{\text{out}}^0)'(0) \neq 0$, hence the number of nonzero unstable roots of D_{in}^0 , D_{out} , D_{out}^0 is even.*

Finally, we have the following auxiliary results established by energy estimates in Appendices C, D, E, and F.

Proposition 3.6. *The limiting Evans function D_{in}^0 is nonzero for $\lambda \neq 0$ on $\Re\lambda \geq 0$, for all $1 > v_0 > 0$. The limiting Evans function D_{out}^0 is nonzero for $\lambda \neq 0$ on $\Re\lambda \geq 0$, for $1 > v_0 > v_*$, where $v_* \approx 0.0899$ is determined by the functional equation $v_* = e^{-2/(1-v_*)^2}$.*

Proposition 3.7. *Compressive outflow boundary layers are stable for v_+ sufficiently close to 1.*

Proposition 3.8 ([19]). *Expansive inflow boundary layers are stable for all parameter values.*

Collecting information, we have the following analytical stability results.

³Indeed, these may be deduced from the results of [25], taking account of the difference between Eulerian and Lagrangian coordinates.

Corollary 3.9. *For v_0 or v_+ sufficiently small, compressive inflow boundary layers are stable. For v_0 sufficiently small, v_+ sufficiently close to 1, or $v_0 > v_* \approx .0899$ and v_+ sufficiently small, compressive outflow layers are stable. Expansive inflow boundary layers are stable for all parameter values.*

Stability of inflow boundary layers in the characteristic limit $v_+ \rightarrow 1$ is not treated here, but should be treatable analytically by the asymptotic ODE methods used in [22, 7] to study the small-amplitude (characteristic) shock limit. This would be an interesting direction for future investigation. The characteristic limit is not accessible numerically, since the exponential decay rate of the background profile decays to zero as $|1 - v_+|$, so that the numerical domain of integration needed to resolve the eigenvalue ODE becomes infinitely large as $v_+ \rightarrow 1$.

Remark 3.10. *Stability in the noncharacteristic weak layer limit $v_0 \rightarrow v_+$ [resp. 1] in the inflow [outflow] case, for v_+ bounded away from the strong and characteristic limits 0 and 1 has already been established in [10, 23]. Indeed, it is shown in [10] that the Evans function converges to that for a constant solution, and this is a regular perturbation.*

Remark 3.11. *Stability of $D_{\text{in}}^0, D_{\text{out}}^0$ may also be determined numerically, in particular in the region $v_0 \leq v_*$ not covered by Proposition 3.6.*

3.3. Numerical results. The asymptotic results of Section 3.2 reduce the problem of (uniformly noncharacteristic, v_+ bounded away from $v_- = 1$) boundary layer stability to a bounded parameter range on which the Evans function may be efficiently computed numerically in a way that is uniformly well-conditioned; see [5]. Specifically, we may map a semicircle

$$\partial\{\Re\lambda \geq 0\} \cap \{|\lambda| \leq 10\}$$

enclosing Λ for $\gamma \in [1, 3]$ by $D_{\text{in}}^0, D_{\text{out}}^0, D_{\text{in}}, D_{\text{out}}$ and compute the winding number of its image about the origin to determine the number of zeroes of the various Evans functions within the semicircle, and thus within Λ . For details of the numerical algorithm, see [3, 5].

In all cases, we obtain results consistent with stability; that is, a winding number of zero or one, depending on the situation. In the case of a single nonzero root, we know from our limiting analysis that this root may be quite near $\lambda = 0$, making delicate the direct determination of its stability; however, in this case we do not attempt to determine the stability numerically, but rely on the analytically computed stability index to conclude stability. See Section 6 for further details.

3.4. Conclusions. As in the shock case [3, 12], our results indicate *unconditional stability* of uniformly noncharacteristic boundary-layers for isentropic Navier–Stokes equations (and, for outflow layer, in the characteristic limit as well), despite the additional complexity of the boundary-layer case. However, two additional comments are in order, perhaps related. First, we point out that the apparent symmetry of Theorem 3.3 in the $v_0 \rightarrow 0$ outflow and

$v_0 \rightarrow 1$ inflow limits is somewhat misleading. For, the limiting, shock Evans function possesses a single zero at $\lambda = 0$, indicating that stability of inflow boundary layers is somewhat delicate as $v_0 \rightarrow 1$: specifically, they have an eigenvalue near zero, which, though stable, is (since vanishingly small in the shock limit) not “very” stable. Likewise, the limiting Evans function D_{in}^0 as $v_+ \rightarrow 0$ possesses a zero at $\lambda = 0$, with the same conclusions.

By contrast, the Evans functions of outflow boundary layers possess a spurious zero at $\lambda = 0$, so that convergence to the shock or strong-layer limit in this case implies the *absence* of any eigenvalues near zero, or “uniform” stability as $v_+ \rightarrow 0$. In this sense, strong outflow boundary layers appear to be more stable than inflow boundary layers. One may make interesting comparisons to physical attempts to stabilize laminar flow along an air- or hydro-foil by suction (outflow) along the boundary. See, for example, the interesting treatise [24].

Second, we point out the result of *instability* obtained in [25] for inflow boundary-layers of the full (nonisentropic) ideal-gas equations for appropriate ratio of the coefficients of viscosity and heat conduction. This suggests that the small eigenvalues of the strong inflow-layer limit may in some cases perturb to the unstable side. It would be very interesting to make these connections more precise, as we hope to do in future work.

4. BOUNDARY-LAYER ANALYSIS

Since the structure of (34) is essentially the same as that of the shock case, we may follow exactly the treatment in [12] analyzing the flow of (34) in the singular region $x \rightarrow +\infty$. As we shall need the details for further computations (specifically, the proof of Theorem 3.4), we repeat the analysis here in full.

Our starting point is the observation that

$$(54) \quad A(x, \lambda) = \begin{pmatrix} 0 & \lambda & \lambda \\ 0 & 0 & \lambda \\ \hat{v} & \hat{v} & f(\hat{v}) - \lambda \end{pmatrix}$$

is approximately block upper-triangular for \hat{v} sufficiently small, with diagonal blocks $\begin{pmatrix} 0 & \lambda \\ 0 & 0 \end{pmatrix}$ and $(f(\hat{v}) - \lambda)$ that are uniformly spectrally separated on $\Re e \lambda \geq 0$, as follows by

$$(55) \quad f(\hat{v}) \leq \hat{v} - 1 \leq -3/4.$$

We exploit this structure by a judicious coordinate change converting (34) to a system in exact upper triangular form, for which the decoupled “slow” upper lefthand 2×2 block undergoes a *regular perturbation* that can be analyzed by standard tools introduced in [22]. Meanwhile, the fast, lower righthand 1×1 block, since scalar, may be solved exactly.

4.1. Preliminary transformation. We first block upper-triangularize by a static (constant) coordinate transformation the limiting matrix

$$(56) \quad A_+ = A(+\infty, \lambda) = \begin{pmatrix} 0 & \lambda & \lambda \\ 0 & 0 & \lambda \\ v_+ & v_+ & f(v_+) - \lambda \end{pmatrix}$$

at $x = +\infty$ using special block lower-triangular transformations

$$(57) \quad R_+ := \begin{pmatrix} I & 0 \\ v_+\theta_+ & 1 \end{pmatrix}, \quad L_+ := R_+^{-1} = \begin{pmatrix} I & 0 \\ -v_+\theta_+ & 1 \end{pmatrix},$$

where I denotes the 2×2 identity matrix and $\theta_+ \in \mathbb{C}^{1 \times 2}$ is a 1×2 row vector.

Lemma 4.1. *On any compact subset of $\Re e \lambda \geq 0$, for each $v_+ > 0$ sufficiently small, there exists a unique $\theta_+ = \theta_+(v_+, \lambda)$ such that $\hat{A}_+ := L_+ A_+ R_+$ is upper block-triangular,*

$$(58) \quad \hat{A}_+ = \begin{pmatrix} \lambda(J + v_+\mathbb{1}\theta_+) & \lambda\mathbb{1} \\ 0 & f(v_+) - \lambda - \lambda v_+\theta_+\mathbb{1} \end{pmatrix},$$

where $J = \begin{pmatrix} 0 & 1 \\ 0 & 0 \end{pmatrix}$ and $\mathbb{1} = \begin{pmatrix} 1 \\ 1 \end{pmatrix}$, satisfying a uniform bound

$$(59) \quad |\theta_+| \leq C.$$

Proof. Setting the $2-1$ block of \hat{A}_+ to zero, we obtain the matrix equation

$$\theta_+(aI - \lambda J) = -\mathbb{1}^T + \lambda v_+\theta_+\mathbb{1}\theta_+,$$

where $a = f(v_+) - \lambda$, or, equivalently, the fixed-point equation

$$(60) \quad \theta_+ = (aI - \lambda J)^{-1} \left(-\mathbb{1}^T + \lambda v_+\theta_+\mathbb{1}\theta_+ \right).$$

By $\det(aI - \lambda J) = a^2 \neq 0$, $(aI - \lambda J)^{-1}$ is uniformly bounded on compact subsets of $\Re e \lambda \geq 0$ (indeed, it is uniformly bounded on all of $\Re e \lambda \geq 0$), whence, for $|\lambda|$ bounded and v_+ sufficiently small, there exists a unique solution by the Contraction Mapping Theorem, which, moreover, satisfies (59). \square

4.2. Dynamic triangularization. Defining now $Y := L_+ W$ and

$$\hat{A}(x, \lambda) = L_+ A(x, \lambda) R_+(x, \lambda) = \begin{pmatrix} \lambda(J + v_+\mathbb{1}\theta_+) & \lambda\mathbb{1} \\ (\hat{v} - v_+)\mathbb{1}^T - v_+(f(\hat{v}) - f(v_+))\theta_+ & f(\hat{v}) - \lambda - \lambda v_+\theta_+\mathbb{1} \end{pmatrix},$$

we have converted (34) to an asymptotically block upper-triangular system

$$(61) \quad Y' = \hat{A}(x, \lambda)Y,$$

with $\hat{A}_+ = \hat{A}(+\infty, \lambda)$ as in (58). Our next step is to choose a *dynamic* transformation of the same form

$$(62) \quad \tilde{R} := \begin{pmatrix} I & 0 \\ \tilde{\Theta} & 1 \end{pmatrix}, \quad \tilde{L} := \tilde{R}^{-1} = \begin{pmatrix} I & 0 \\ -\tilde{\Theta} & 1 \end{pmatrix},$$

converting (61) to an exactly block upper-triangular system, with $\tilde{\Theta}$ uniformly exponentially decaying at $x = +\infty$: that is, a *regular perturbation* of the identity.

Lemma 4.2. *On any compact subset of $\Re\lambda \geq 0$, for L sufficiently large and each $v_+ > 0$ sufficiently small, there exists a unique $\Theta = \Theta_+(x, \lambda, v_+)$ such that $\tilde{A} := \tilde{L}\hat{A}(x, \lambda)\tilde{R} + \tilde{L}'\tilde{R}$ is upper block-triangular,*

$$(63) \quad \tilde{A} = \begin{pmatrix} \lambda(J + v_+ \mathbb{1}\theta_+ + \mathbb{1}\tilde{\Theta}) & \lambda\mathbb{1} \\ 0 & f(\hat{v}) - \lambda - \lambda\theta_+ \mathbb{1} - \lambda\tilde{\Theta}\mathbb{1} \end{pmatrix},$$

and $\tilde{\Theta}(L) = 0$, satisfying a uniform bound

$$(64) \quad |\tilde{\Theta}(x, \lambda, v_+)| \leq Ce^{-\eta x}, \quad \eta > 0, \quad x \geq L,$$

independent of the choice of L, v_+ .

Proof. Setting the 2 – 1 block of \tilde{A} to zero and computing

$$\tilde{L}'\tilde{R} = \begin{pmatrix} 0 & 0 \\ -\tilde{\Theta}' & 0 \end{pmatrix} \begin{pmatrix} I & 0 \\ \tilde{\Theta} & I \end{pmatrix} = \begin{pmatrix} 0 & 0 \\ -\tilde{\Theta}' & 0 \end{pmatrix},$$

we obtain the matrix equation

$$(65) \quad \tilde{\Theta}' - \tilde{\Theta}(aI - \lambda(J + v_+ \mathbb{1}\theta_+)) = \zeta + \lambda\tilde{\Theta}\mathbb{1}\tilde{\Theta},$$

where $a(x) := f(\hat{v}) - \lambda - \lambda v_+ \theta_+ \mathbb{1}$ and the forcing term

$$\zeta := -(\hat{v} - v_+) \mathbb{1}^T + v_+(f(\hat{v}) - f(v_+))\theta_+$$

by derivative estimate $df/d\hat{v} \leq C\hat{v}^{-1}$ together with the Mean Value Theorem is uniformly exponentially decaying:

$$(66) \quad |\zeta| \leq C|\hat{v} - v_+| \leq C_2e^{-\eta x}, \quad \eta > 0.$$

Initializing $\tilde{\Theta}(L) = 0$, we obtain by Duhamel's Principle/Variation of Constants the representation (suppressing the argument λ)

$$(67) \quad \tilde{\Theta}(x) = \int_L^x S^{y \rightarrow x} (\zeta + \lambda\tilde{\Theta}\mathbb{1}\tilde{\Theta})(y) dy,$$

where $S^{y \rightarrow x}$ is the solution operator for the homogeneous equation

$$\tilde{\Theta}' - \tilde{\Theta}(aI - \lambda(J + v_+ \mathbb{1}\theta_+)) = 0,$$

or, explicitly,

$$S^{y \rightarrow x} = e^{\int_y^x a(y) dy} e^{-\lambda(J + v_+ \mathbb{1}\theta_+)(x-y)}.$$

For $|\lambda|$ bounded and v_+ sufficiently small, we have by matrix perturbation theory that the eigenvalues of $-\lambda(J + v_+ \mathbb{1}\theta_+)$ are small and the entries are bounded, hence

$$|e^{-\lambda(J + v_+ \mathbb{1}\theta_+)z}| \leq Ce^{\epsilon z}$$

for $z \geq 0$. Recalling the uniform spectral gap $\Re a = f(\hat{v}) - \Re \lambda \leq -1/2$ for $\Re \lambda \geq 0$, we thus have

$$(68) \quad |S^{y \rightarrow x}| \leq C e^{\eta(x-y)}$$

for some $C, \eta > 0$. Combining (66) and (68), we obtain

$$(69) \quad \left| \int_L^x S^{y \rightarrow x} \zeta(y) dy \right| \leq \int_L^x C_2 e^{-\eta(x-y)} e^{-(\eta/2)y} dy \\ = C_3 e^{-(\eta/2)x}.$$

Defining $\tilde{\Theta}(x) =: \tilde{\theta}(x) e^{-(\eta/2)x}$ and recalling (67) we thus have

$$(70) \quad \tilde{\theta}(x) = f + e^{(\eta/2)x} \int_L^x S^{y \rightarrow x} e^{-\eta y} \lambda \tilde{\theta} \mathbb{1} \tilde{\theta}(y) dy,$$

where $f := e^{(\eta/2)x} \int_L^x S^{y \rightarrow x} \zeta(y) dy$ is uniformly bounded, $|f| \leq C_3$, and $e^{(\eta/2)x} \int_L^x S^{y \rightarrow x} e^{-\eta y} \lambda \tilde{\theta} \mathbb{1} \tilde{\theta}(y) dy$ is contractive with arbitrarily small contraction constant $\epsilon > 0$ in $L^\infty[L, +\infty)$ for $|\tilde{\theta}| \leq 2C_3$ for L sufficiently large, by the calculation

$$\left| e^{(\eta/2)x} \int_L^x S^{y \rightarrow x} e^{-\eta y} \lambda \tilde{\theta}_1 \mathbb{1} \tilde{\theta}_1(y) - e^{(\eta/2)x} \int_L^x S^{y \rightarrow x} e^{-\eta y} \lambda \tilde{\theta}_2 \mathbb{1} \tilde{\theta}_2(y) \right| \\ \leq \left| e^{(\eta/2)x} \int_L^x C e^{-\eta(x-y)} e^{-\eta y} dy \right| |\lambda| \|\tilde{\theta}_1 - \tilde{\theta}_2\|_\infty \max_j \|\tilde{\theta}_j\|_\infty \\ \leq e^{-(\eta/2)L} \left| \int_L^x C e^{-(\eta/2)(x-y)} dy \right| |\lambda| \|\tilde{\theta}_1 - \tilde{\theta}_2\|_\infty \max_j \|\tilde{\theta}_j\|_\infty \\ = C_3 e^{-(\eta/2)L} |\lambda| \|\tilde{\theta}_1 - \tilde{\theta}_2\|_\infty \max_j \|\tilde{\theta}_j\|_\infty.$$

It follows by the Contraction Mapping Principle that there exists a unique solution $\tilde{\theta}$ of fixed point equation (70) with $|\tilde{\theta}(x)| \leq 2C_3$ for $x \geq L$, or, equivalently (redefining the unspecified constant η), (64). \square

4.3. Fast/Slow dynamics. Making now the further change of coordinates

$$Z = \tilde{L}Y$$

and computing

$$(\tilde{L}Y)' = \tilde{L}Y' + \tilde{L}'Y = (\tilde{L}A_+ + \tilde{L}'Y), \\ = (\tilde{L}A_+ \tilde{R} + \tilde{L}'\tilde{R})Z,$$

we find that we have converted (61) to a block-triangular system

$$(71) \quad Z' = \tilde{A}Z = \begin{pmatrix} \lambda(J + v_+ \mathbb{1} \theta_+ + \mathbb{1} \tilde{\Theta}) & \lambda \mathbb{1} \\ 0 & f(\hat{v}) - \lambda - \lambda v_+ \theta_+ \mathbb{1} - \lambda \tilde{\Theta} \mathbb{1} \end{pmatrix} Z,$$

related to the original eigenvalue system (34) by

$$(72) \quad W = LZ, \quad R := R_+ R = \begin{pmatrix} I & 0 \\ \Theta & 1 \end{pmatrix}, \quad L := R^{-1} = \begin{pmatrix} I & 0 \\ -\Theta & 1 \end{pmatrix},$$

where

$$(73) \quad \Theta = \tilde{\Theta} + v_+ \theta_+.$$

Since it is triangular, (71) may be solved completely if we can solve the component systems associated with its diagonal blocks. The *fast system*

$$z' = \left(f(\hat{v}) - \lambda - \lambda v_+ \theta_+ \mathbb{1} - \lambda \tilde{\Theta} \mathbb{1} \right) z$$

associated to the lower righthand block features rapidly-varying coefficients. However, because it is scalar, it can be solved explicitly by exponentiation.

The *slow system*

$$(74) \quad z' = \lambda(J + v_+ \mathbb{1} \theta_+ + \mathbb{1} \tilde{\Theta}) z$$

associated to the upper lefthand block, on the other hand, by (64), is an exponentially decaying perturbation of a constant-coefficient system

$$(75) \quad z' = \lambda(J + v_+ \mathbb{1} \theta_+) z$$

that can be explicitly solved by exponentiation, and thus can be well-estimated by comparison with (75). A rigorous version of this statement is given by the *conjugation lemma* of [20]:

Proposition 4.3 ([20]). *Let $M(x, \lambda) = M_+(\lambda) + \Theta(x, \lambda)$, with M_+ continuous in λ and $|\Theta(x, \lambda)| \leq C e^{-\eta x}$, for λ in some compact set Λ . Then, there exists a globally invertible matrix $P(x, \lambda) = I + Q(x, \lambda)$ such that the coordinate change $z = Pv$ converts the variable-coefficient ODE $z' = M(x, \lambda)z$ to a constant-coefficient equation*

$$v' = M_+(\lambda)v,$$

satisfying for any L , $0 < \hat{\eta} < \eta$ a uniform bound

$$(76) \quad |Q(x, \lambda)| \leq C(L, \hat{\eta}, \eta, \max |(M_+)_{ij}|, \dim M_+) e^{-\hat{\eta} x} \quad \text{for } x \geq L.$$

Proof. See [20, 27], or Appendix C, [12]. □

By Proposition 4.3, the solution operator for (74) is given by

$$(77) \quad P(y, \lambda) e^{\lambda(J + v_+ \mathbb{1} \theta_+(\lambda, v_+))(x-y)} P(x, \lambda)^{-1},$$

where P is a uniformly small perturbation of the identity for $x \geq L$ and $L > 0$ sufficiently large.

5. PROOF OF THE MAIN THEOREMS

With these preparations, we turn now to the proofs of the main theorems.

5.1. Boundary estimate. We begin by recalling the following estimates established in [12] on $\widetilde{W}_1^+(L + \delta)$, that is, the value of the dual mode \widetilde{W}_1^+ appearing in (42) at the boundary $x = L + \delta$ between regular and singular regions. For completeness, and because we shall need the details in further computations, we repeat the proof in full.

Lemma 5.1 ([12]). *For λ on any compact subset of $\Re\lambda \geq 0$, and $L > 0$ sufficiently large, with \widetilde{W}_1^+ normalized as in [8, 22, 3],*

$$(78) \quad |\widetilde{W}_1^+(L + \delta) - \widetilde{V}_1| \leq Ce^{-\eta L}$$

as $v_+ \rightarrow 0$, uniformly in λ , where $C, \eta > 0$ are independent of L and

$$\widetilde{V}_1 := (0, -1, \lambda/\mu)^T$$

is the limiting direction vector (53) appearing in the definition of D_{in}^0 .

Corollary 5.2 ([12]). *Under the hypotheses of Lemma 5.1,*

$$(79) \quad |\widetilde{W}_1^{0+}(L + \delta) - \widetilde{V}_1| \leq Ce^{-\eta L}$$

and

$$(80) \quad |\widetilde{W}_1^+(L + \delta) - \widetilde{W}_1^{0+}(L + \delta)| \leq Ce^{-\eta L}$$

as $v_+ \rightarrow 0$, uniformly in λ , where $C, \eta > 0$ are independent of L and \widetilde{W}_1^{0+} is the solution of the limiting adjoint eigenvalue system appearing in definition (52) of D^0 .

Proof of Lemma 5.1. First, make the independent coordinate change $x \rightarrow x - \delta$ normalizing the background wave to match the shock-wave case. Making the dependent coordinate-change

$$(81) \quad \widetilde{Z} := R^* \widetilde{W},$$

R as in (72), reduces the adjoint equation $\widetilde{W}' = -A^* \widetilde{W}$ to block lower-triangular form,

$$(82) \quad \widetilde{Z}' = -\widetilde{A}^* \widetilde{Z} = \begin{pmatrix} -\bar{\lambda}(J^T + v_+ \mathbb{1} \theta_+ + \mathbb{1} \widetilde{\Theta})^* & 0 \\ -\bar{\lambda} \mathbb{1}^T & -f(\hat{v}) + \bar{\lambda} + \bar{\lambda} v_+ (\theta_+ \mathbb{1} + \widetilde{\Theta} \mathbb{1})^* \end{pmatrix} \widetilde{Z},$$

with “ $-$ ” denoting complex conjugate.

Denoting by \widetilde{V}_1^+ a suitably normalized element of the one-dimensional (slow) stable subspace of $-\widetilde{A}^*$, we find readily (see [12] for further discussion) that, without loss of generality,

$$(83) \quad \widetilde{V}_1^+ \rightarrow (0, 1, \bar{\lambda}(\gamma + \bar{\lambda})^{-1})^T$$

as $v_+ \rightarrow 0$, while the associated eigenvalue $\tilde{\mu}_1^+ \rightarrow 0$, uniformly for λ on an compact subset of $\Re\lambda \geq 0$. The dual mode $\widetilde{Z}_1^+ = R^* \widetilde{W}_1^+$ is uniquely determined by the property that it is asymptotic as $x \rightarrow +\infty$ to the corresponding constant-coefficient solution $e^{\tilde{\mu}_1^+ x} \widetilde{V}_1^+$ (the standard normalization of [8, 22, 3]).

By lower block-triangular form (82), the equations for the slow variable $\tilde{z}^T := (\tilde{Z}_1, \tilde{Z}_2)$ decouples as a slow system

$$(84) \quad \tilde{z}' = -\left(\lambda(J + v_+ \mathbb{1}\theta_+ + \mathbb{1}\tilde{\Theta})\right)^* \tilde{z}$$

dual to (74), with solution operator

$$(85) \quad P^*(x, \lambda)^{-1} e^{-\bar{\lambda}(J+v_+ \mathbb{1}\theta_+)^*(x-y)} P(y, \lambda)^*$$

dual to (77), i.e. (fixing $y = L$, say), solutions of general form

$$(86) \quad \tilde{z}(\lambda, x) = P^*(x, \lambda)^{-1} e^{-\bar{\lambda}(J+v_+ \mathbb{1}\theta_+)^*(x-y)} \tilde{v},$$

$\tilde{v} \in \mathbb{C}^2$ arbitrary.

Denoting by

$$\tilde{Z}_1^+(L) := R^* \tilde{W}_1^+(L),$$

therefore, the unique (up to constant factor) decaying solution at $+\infty$, and $\tilde{v}_1^+ := ((\tilde{V}_1^+)_1, (\tilde{V}_1^+)_2)^T$, we thus have evidently

$$\tilde{z}_1^+(x, \lambda) = P^*(x, \lambda)^{-1} e^{-\bar{\lambda}(J+v_+ \mathbb{1}\theta_+)^*(x-y)} \tilde{v}_1^+,$$

which, as $v_+ \rightarrow 0$, is uniformly bounded by

$$(87) \quad |\tilde{z}_1^+(x, \lambda)| \leq C e^{\epsilon x}$$

for arbitrarily small $\epsilon > 0$ and, by (83), converges for x less than or equal to $X - \delta$ for any fixed X simply to

$$(88) \quad \lim_{v_+ \rightarrow 0} \tilde{z}_1^+(x, \lambda) = P^*(x, \lambda)^{-1} (0, 1)^T.$$

Defining by $\tilde{q} := (\tilde{Z}_1^+)_3$ the fast coordinate of \tilde{Z}_1^+ , we have, by (82),

$$\tilde{q}' + \left(f(\hat{v}) - \bar{\lambda} - (\lambda v_+ \theta_+ \mathbb{1} + \lambda \tilde{\Theta} \mathbb{1})^*\right) \tilde{q} = \bar{\lambda} \mathbb{1}^T \tilde{z}_1^+,$$

whence, by Duhamel's principle, any decaying solution is given by

$$\tilde{q}(x, \lambda) = \int_x^{+\infty} e^{\int_y^x a(z, \lambda, v_+) dz} \bar{\lambda} \mathbb{1}^T z_1^+(y) dy,$$

where

$$a(y, \lambda, v_+) := -\left(f(\hat{v}) - \bar{\lambda} - (\lambda v_+ \theta_+ \mathbb{1} + \lambda \tilde{\Theta} \mathbb{1})^*\right).$$

Recalling, for $\Re e \lambda \geq 0$, that $\Re e a \geq 1/2$, combining (87) and (88), and noting that a converges uniformly on $y \leq Y$ as $v_+ \rightarrow 0$ for any $Y > 0$ to

$$\begin{aligned} a_0(y, \lambda) &:= -f_0(\hat{v}) + \bar{\lambda} + (\lambda \tilde{\Theta}_0 \mathbb{1})^* \\ &= (1 + \bar{\lambda}) + O(e^{-\eta y}) \end{aligned}$$

we obtain by the Lebesgue Dominated Convergence Theorem that

$$\begin{aligned}\tilde{q}(L, \lambda) &\rightarrow \int_L^{+\infty} e^{\int_y^L a_0(z, \lambda) dz} \bar{\lambda} \mathbb{1}^T(0, 1)^T dy \\ &= \bar{\lambda} \int_L^{+\infty} e^{(1+\bar{\lambda})(L-y) + \int_y^L O(e^{-\eta z}) dz} dy \\ &= \bar{\lambda}(1 + \bar{\lambda})^{-1}(1 + O(e^{-\eta L})).\end{aligned}$$

Recalling, finally, (88), and the fact that

$$|P - Id|(L, \lambda), |R - Id|(L, \lambda) \leq Ce^{-\eta L}$$

for v_+ sufficiently small, we obtain (78) as claimed. \square

Proof of Corollary 5.2. Again, make the coordinate change $x \rightarrow x - \delta$ normalizing the background wave to match the shock-wave case. Applying Proposition 4.3 to the limiting adjoint system

$$\tilde{W}' = -(A^0)^* \tilde{W} = \begin{pmatrix} 0 & 0 & 0 \\ -\bar{\lambda} & 0 & 0 \\ -1 & -1 & 1 + \bar{\lambda} \end{pmatrix} \tilde{W} + O(e^{-\eta x}) \tilde{W},$$

we find that, up to an $Id + O(e^{-\eta x})$ coordinate change, $\tilde{W}_1^{0+}(x)$ is given by the exact solution $\tilde{W} \equiv \tilde{V}_1$ of the limiting, constant-coefficient system

$$\tilde{W}' = -(A^0)^* \tilde{W} = \begin{pmatrix} 0 & 0 & 0 \\ -\bar{\lambda} & 0 & 0 \\ -1 & -1 & 1 + \bar{\lambda} \end{pmatrix} \tilde{W}.$$

This yields immediately (79), which, together with (78), yields (80). \square

5.2. Convergence to D^0 . The rest of our analysis is standard.

Lemma 5.3. *On $x \leq L - \delta$ for any fixed $L > 0$, there exists a coordinate-change $W = TZ$ conjugating (34) to the limiting equations (50), $T = T(x, \lambda, v_+)$, satisfying a uniform bound*

$$(89) \quad |T - Id| \leq C(L)v_+$$

for all $v_+ > 0$ sufficiently small.

Proof. Make the coordinate change $x \rightarrow x - \delta$ normalizing the background profile. For $x \in (-\infty, 0]$, this is a consequence of the *Convergence Lemma* of [22], a variation on Proposition 4.3, together with uniform convergence of the profile and eigenvalue equations. For $x \in [0, L]$, it is essentially continuous dependence; more precisely, observing that $|A - A^0| \leq C_1(L)v_+$ for $x \in [0, L]$, setting $S := T - Id$, and writing the homological equation expressing conjugacy of (34) and (50), we obtain

$$S' - (AS - SA^0) = (A - A^0),$$

which, considered as an inhomogeneous linear matrix-valued equation, yields an exponential growth bound

$$S(x) \leq e^{Cx}(S(0) + C^{-1}C_1(L)v_+)$$

for some $C > 0$, giving the result. \square

Proof of Theorem 3.2: inflow case. Make the coordinate change $x \rightarrow x - \delta$ normalizing the background profile. Lemma 5.3, together with convergence as $v_+ \rightarrow 0$ of the unstable subspace of A_- to the unstable subspace of A_-^0 at the same rate $O(v_+)$ (as follows by spectral separation of the unstable eigenvalue of A^0 and standard matrix perturbation theory) yields

$$(90) \quad |W_1^0(0, \lambda) - W_1^{00}(0, \lambda)| \leq C(L)v_+.$$

Likewise, Lemma 5.3 gives

$$(91) \quad |\tilde{W}_1^+(0, \lambda) - \tilde{W}_1^{0+}(0, \lambda)| \leq C(L)v_+|\tilde{W}_1^+(0, \lambda)| \\ + |S_0^{L \rightarrow 0}| |\tilde{W}_1^+(L, \lambda) - \tilde{W}_1^{0+}(L, \lambda)|,$$

where $S_0^{y \rightarrow x}$ denotes the solution operator of the limiting adjoint eigenvalue equation $\tilde{W}' = -(A^0)^* \tilde{W}$. Applying Proposition 4.3 to the limiting system, we obtain

$$|S_0^{L \rightarrow 0}| \leq C_2 e^{-A_+^0 L} \leq C_2 L |\lambda|$$

by direct computation of $e^{-A_+^0 L}$, where C_2 is independent of $L > 0$. Together with (80) and (91), this gives

$$|\tilde{W}_1^+(0, \lambda) - \tilde{W}_1^{0+}(0, \lambda)| \leq C(L)v_+|\tilde{W}_1^+(0, \lambda)| + L|\lambda|C_2 C e^{-\eta L},$$

hence, for $|\lambda|$ bounded,

$$(92) \quad |\tilde{W}_1^+(0, \lambda) - \tilde{W}_1^{0+}(0, \lambda)| \leq C_3(L)v_+|\tilde{W}_1^{0+}(0, \lambda)| + LC_4 e^{-\eta L} \\ \leq C_5(L)v_+ + LC_4 e^{-\eta L}.$$

Taking first $L \rightarrow \infty$ and then $v_+ \rightarrow 0$, we obtain therefore convergence of $W_1^+(0, \lambda)$ and $\tilde{W}_1^+(0, \lambda)$ to $W_1^{0+}(0, \lambda)$ and $\tilde{W}_1^{0+}(0, \lambda)$, yielding the result by definitions (42) and (52). \square

Proof of Theorem 3.2: outflow case. Straightforward, following the previous argument in the regular region only. \square

5.3. Convergence to the shock case.

Proof of Theorem 3.4: inflow case. First make the coordinate change $x \rightarrow x - \delta$ normalizing the background profile location to that of the shock wave case, where $\delta \rightarrow +\infty$ as $v_0 \rightarrow 1$. By standard duality properties,

$$D_{\text{in}} = W_1^0 \cdot \tilde{W}_1^+|_{x=x_0}$$

is independent of x_0 , so we may evaluate at $x = 0$ as in the shock case. Denote by $\mathcal{W}_1^-, \tilde{\mathcal{W}}_1^+$ the corresponding modes in the shock case, and

$$\mathcal{D} = \mathcal{W}_1^- \cdot \tilde{\mathcal{W}}_1^+|_{x=0}$$

the resulting Evans function.

Noting that $\tilde{\mathcal{W}}_+^1$ and \tilde{W}_+^1 are asymptotic to the unique stable mode at $+\infty$ of the (same) adjoint eigenvalue equation, but with translated decay rates, we see immediately that $\tilde{\mathcal{W}}_+^1 = \tilde{W}_+^1 e^{-\delta \bar{\mu}_+^1}$. W_1^0 on the other hand is initialized at $x = -\delta$ (in the new coordinates $\tilde{x} = x - \delta$) as

$$W_1^0(-\delta) = (1, 0, 0)^T,$$

whereas \mathcal{W}_1^- is the unique unstable mode at $-\infty$ decaying as $e^{\mu_1^- x} V_1^-$, where V_1^- is the unstable right eigenvector of

$$A_- = \begin{pmatrix} 0 & \lambda & \lambda \\ 0 & 0 & \lambda \\ 1 & 1 & f(1) - \lambda \end{pmatrix}.$$

Denote by \tilde{V}_1^- the associated dual unstable left eigenvector and

$$\Pi_1^- := V_1^- (\tilde{V}_1^-)^T$$

the eigenprojection onto the stable vector V_1^- . By direct computation,

$$\tilde{V}_1^- = c(\lambda)(1, 1 + \lambda/\mu_1^-, \mu_1^-)^T, \quad c(\lambda) \neq 0,$$

yielding

$$(93) \quad \Pi_1^- W_1^0 =: \beta(\lambda) = c(\lambda) \neq 0$$

for $\Re \lambda \geq 0$, on which $\Re \mu_1^- > 0$.

Once we know (93), we may finish by a standard argument, concluding by exponential attraction in the positive x -direction of the unstable mode that other modes decay exponentially as $x \rightarrow 0$, leaving the contribution from $\beta(\lambda)V_1^-$ plus a negligible $O(e^{-\eta\delta})$ error, $\eta > 0$, from which we may conclude that $\mathcal{W}_1^-|_{x=0} \sim \beta^{-1} e^{-\delta \mu_1^-} W_1^0|_{x=0}$. Collecting information, we find that

$$\mathcal{D}(\lambda) = \beta(\lambda)^{-1} e^{-\delta(\bar{\mu}_1^- + \bar{\mu}_1^+)(\lambda)} D_{\text{in}}(\lambda) + O(e^{-\eta\delta}),$$

$\eta > 0$, yielding the claimed convergence as $v_0 \rightarrow 1$, $\delta \rightarrow +\infty$. \square

Proof of Theorem 3.4: outflow case. For λ uniformly bounded from zero, $\tilde{W}_1^0 = (0, -1, -\bar{\lambda}/(\bar{\lambda} - \hat{v}'(0)))^T$ converges uniformly as $v_0 \rightarrow 0$ to

$$(0, -1, -1)^T,$$

whereas the shock Evans function \mathcal{D} is initiated by $\tilde{\mathcal{W}}_1^+$ proportional to

$$\tilde{\mathcal{V}}_1^+ = (0, -1, -1 - \lambda)^T$$

agreeing in the first two coordinates with \tilde{W}_1^0 . By the boundary-layer analysis of Section 5.1, the backward (i.e., decreasing x) evolution of the adjoint eigenvalue ODE reduces in the asymptotic limit $v_+ \rightarrow 0$ (forced by $v_0 \rightarrow 0$) to a decoupled slow flow

$$\tilde{w}' = \begin{pmatrix} 0 & \bar{\lambda} \\ 0 & 0 \end{pmatrix} w, \quad w \in \mathbb{C}^2$$

in the first two coordinates, driving an exponentially slaved fast flow in the third coordinate. From this, we may conclude that solutions agreeing in the first two coordinates converge exponentially as x decreases. Performing an appropriate normalization, as in the inflow case just treated, we thus obtain the result. We omit the details, which follow what has already been done in previous cases. \square

5.4. The stability index. Following [25, 10], we note that $D_{\text{in}}(\lambda)$ is real for real λ , and nonvanishing for real λ sufficiently large, hence $\text{sgn}D_{\text{in}}(+\infty)$ is well-defined and constant on the entire (connected) parameter range. The number of roots of D_{in} on $\Re\lambda \geq 0$ is therefore even or odd depending on the *stability index*

$$\text{sgn}[D_{\text{in}}(0)D_{\text{in}}(+\infty)].$$

Similarly, recalling that $D_{\text{out}}(0) \equiv 0$, we find that the number of roots of D_{out} on $\Re\lambda \geq 0$ is even or odd depending on

$$\text{sgn}[D'_{\text{out}}(0)D_{\text{out}}(+\infty)].$$

Proof of Lemma 3.5: inflow case. Examining the adjoint equation at $\lambda = 0$,

$$\tilde{W}' = -A^*\tilde{W}, \quad -A^*(x, 0) = \begin{pmatrix} 0 & 0 & -\hat{v} \\ 0 & 0 & -\hat{v} \\ 0 & 0 & -f(\hat{v}) \end{pmatrix},$$

$-f(v_+) > 0$, we find by explicit computation that the only solutions that are bounded as $x \rightarrow +\infty$ are the *constant solutions* $\tilde{W} \equiv (a, b, 0)^T$. Taking the limit $V_1^+(0)$ as $\lambda \rightarrow 0^+$ along the real axis of the unique stable eigenvector of $-A_+^*(\lambda)$, we find (see, e.g., [27]) that it lies in the direction $(1, 2 + a_j^+, 0)^T$, where $a_j^+ > 0$ is the positive characteristic speed of the hyperbolic convection matrix $\begin{pmatrix} 1 & -1 \\ -h(v_+)/v_+^{\gamma+1} & 1 \end{pmatrix}$, i.e., $V_1^- = c(v_0, v_+)(1, 2 + a_j^+, 0)^T$, $c(v_0, v_+) \neq 0$. Thus, $D_{\text{in}}(0) = V_1^- \cdot (1, 0, 0)^T = \bar{c}(v_0, v_+) \neq 0$ as claimed. On the other hand, the same computation carried out for $D_{\text{in}}^0(0)$ yields $D_{\text{in}}^0(0) \equiv 0$. (Note: $a_j \sim v_+^{-1/2} \rightarrow +\infty$ as $v_+ \rightarrow 0$.) Similarly, as $v_0 \rightarrow 0$,

$$D_{\text{in}}^0(\lambda) \rightarrow (1, 0, 0)^T \cdot (0, 1, *)^T \equiv 0.$$

Finally, note $D_{\text{in}}(0) \neq 0$ implies that the stability index, since continuously varying so long as it doesn't vanish and taking discrete values ± 1 , must be constant on the connected set of parameter values. Since inflow boundary layers are known to be stable on some part of the parameter regime by energy estimates (Theorem 3.4), we may conclude that the stability index is identically one and therefore there are an even number of unstable roots for all $1 > v_0 \geq v_+ > 0$.

To establish that $(D_{\text{in}}^0)'(0) \neq 0$, we compute

$$D_{\text{in}}^0'(0) = (\partial_\lambda W_1^{00}) \cdot \widetilde{W}_1^{0+} + W_1^{00} \cdot (\partial_\lambda \widetilde{W}_1^{0+}).$$

Since $W_1^{00} \equiv (1, 0, 0)$ is independent of λ , we need only show that the first component of $\partial_\lambda \widetilde{W}_1^{0+}$ is nonzero. Note that $\partial_\lambda W_1^{0+}$ solves the limiting adjoint variational equations

$$(\partial_\lambda \widetilde{W}_1^{0+})'(0) + (A^0)^*(x, 0) \partial_\lambda \widetilde{W}_1^{0+} = b(x)$$

with

$$(A^0)^*(x, 0) \equiv \begin{pmatrix} 0 & 0 & \hat{v}^0 \\ 0 & 0 & \hat{v}^0 \\ 0 & 0 & f^0(\hat{v}^0) \end{pmatrix}, \quad b(x) = \begin{pmatrix} 0 \\ \hat{v}^0 + \hat{u}^0 - \frac{\hat{v}^{0'}}{\hat{v}^0} - 1 \\ 3\hat{v}^0 - \frac{\hat{v}^{0'}}{\hat{v}^0} - 1 \end{pmatrix}.$$

By (53), and the fact that $\partial_\lambda \tilde{\mu}_1^{0+} \equiv 0$, $\partial_\lambda \widetilde{W}_1^{0+}(x)$ is chosen so that asymptotically at $x = +\infty$ it lies in the direction of $\partial_\lambda \widetilde{V}_1 = (0, 0, -1)$. Set $\partial_\lambda \widetilde{W}_1^{0+} = (\partial_\lambda \widetilde{W}_{1,1}^{0+}, \partial_\lambda \widetilde{W}_{1,2}^{0+}, \partial_\lambda \widetilde{W}_{1,3}^{0+})^T$. Then the third component solves

$$(\partial_\lambda \widetilde{W}_{1,3}^{0+})' + \hat{v}^0 \partial_\lambda \widetilde{W}_{1,3}^{0+} = b_3 := 3\hat{v}^0 - \frac{\hat{v}^{0'}}{\hat{v}^0} - 1$$

which has solution

$$\partial_\lambda \widetilde{W}_{1,3}^{0+}(x) = \partial_\lambda \widetilde{W}_{1,3}^{0+}(+\infty) \varphi(x) - \varphi(x) \int_x^\infty \varphi^{-1}(y) b_3(y) dy$$

where

$$\varphi(x) = e^{\int_x^\infty \hat{v}^0(y) dy}.$$

Integrating the equation for the first component of $\partial_\lambda \widetilde{W}_1^{0+}$ yields

$$\begin{aligned} \partial_\lambda \widetilde{W}_{1,1}^{0+}(x) &= \partial_\lambda \widetilde{W}_{1,1}^{0+}(+\infty) + \int_x^\infty \partial_\lambda \widetilde{W}_{1,3}^{0+}(y) dy \\ &= \partial_\lambda \widetilde{W}_{1,1}^{0+}(+\infty) + \partial_\lambda \widetilde{W}_{1,3}^{0+}(+\infty) \int_x^\infty \hat{v}^0(y) \varphi(y) dy \\ &\quad - \int_x^\infty \left(\varphi(y) \int_y^\infty \varphi^{-1}(z) b_3(z) dz \right) dy. \end{aligned}$$

Using the condition $\partial_\lambda \widetilde{W}_1^{0+}(+\infty) = (0, 0, -1)^T$ we have $\partial_\lambda \widetilde{W}_{1,1}^{0+}(+\infty) = 0$, $\partial_\lambda \widetilde{W}_{1,3}^{0+}(+\infty) = -1$ so that

$$\partial_\lambda \widetilde{W}_{1,1}^{0+}|_{x=0} = - \int_0^\infty \hat{v}^0(y) \varphi(y) dy - \int_x^\infty \left(\varphi(y) \int_y^\infty \varphi^{-1}(z) b_3 dz \right) dy.$$

Finally, note that by using (49) we have $b_3 = 1 - \tanh(\frac{x-\delta}{2})$ so that for all $x \geq 0$, $\varphi(x), b_3(x) \geq 0$ which implies

$$D_{\text{in}}^0{}'(0) = \partial_\lambda \widetilde{W}_{1,1}^{0+}|_{x=0} \neq 0.$$

□

Remark 5.4. *The result $D_{\text{in}}(0) \neq 0$ at first sight appears to contradict that of Theorem 3.3, since $\mathcal{D}(0) = 0$ for the shock wave case. This apparent contradiction is explained by the fact that the normalizing factor $e^{-\delta(\bar{\mu}_1^- + \bar{\mu}_1^+)}$ is exponentially decaying in δ for $\lambda = 0$, since $\tilde{\mu}_1^+(0) = 0$, while $\Re\mu_1^- > 0$. Recalling that $\delta \rightarrow +\infty$ as $v_0 \rightarrow 1$, we recover the result of Theorem 3.3.*

Proof of Lemma 3.5: outflow case. Similarly, we compute

$$D'_{\text{out}}(0) = \partial\lambda W_1^- \cdot \tilde{W}_1^0,$$

where $\partial\lambda W_1^-|_{\lambda=0}$ satisfies the variational equation $L\partial_\lambda U_1^-(0) = U_1^- = \hat{U}'$, or, written as a first-order system,

$$(\partial\lambda W_1^-)' - A(x, 0)\partial\lambda W_1^- = \begin{pmatrix} \hat{u}_x \\ \hat{v}_x \\ -\hat{v}_x \end{pmatrix}, \quad A(x, 0) = \begin{pmatrix} 0 & 0 & 0 \\ 0 & 0 & 0 \\ \hat{v} & \hat{v} & f(\hat{v}) \end{pmatrix},$$

which may be solved exactly for the unique solution decaying at $-\infty$ of

$$W_1^-(0) = \begin{pmatrix} 0 \\ 0 \\ \hat{v}' \end{pmatrix}, \quad (\partial\lambda W_1^-)(0) = \begin{pmatrix} \hat{u} - u_- \\ \hat{v} - v_- \\ * \end{pmatrix}.$$

Recalling from (47) that $\tilde{W}_1^0(\lambda) = (0, -1, -\lambda/(\lambda - \hat{v}'(0)))^T$, hence

$$\tilde{W}_1^0(0) = (0, -1, 0)^T, \quad \partial_\lambda \tilde{W}_1^0(0) = (0, 0, 1/\hat{v}'(0))^T,$$

we thus find that

$$\begin{aligned} D'_{\text{out}}(0) &= \partial_\lambda W_1^-(0) \cdot \tilde{W}_1^0(0) + W_1^-(0) \cdot \partial_\lambda \tilde{W}_1^0(0) \\ &= -(\hat{v}(0) - 1) + 1 = 2 - v_0 \neq 0 \end{aligned}$$

as claimed. The proof that $(D_{\text{out}}^0)'(0) \neq 0$ goes similarly.

Finally, as in the proof of the inflow case, we note that nonvanishing implies that the stability index is constant across the entire (connected) parameter range, hence we may conclude that it is identically one by existence of a stable case (Corollary 3.9), and therefore that the number of nonzero unstable roots is even, as claimed. \square

5.5. Stability in the shock limit.

Proof of Corollary 3.9: inflow case. By Proposition 3.6 we find that D_{in} has at most a single zero in $\Re\lambda \geq 0$. However, by our stability index results, Theorem 3.5, the number of eigenvalues in $\Re\lambda \geq 0$ is even. Thus, it must be zero, giving the result. \square

Proof of Corollary 3.9: outflow case. By Theorem 3.3, D_{out} , suitably renormalized, converges as $v_0 \rightarrow 0$ to the Evans function for the (unintegrated) shock wave case. But, the shock Evans function by the results of [3, 12] has just a single zero at $\lambda = 0$ on $\Re\lambda \geq 0$, already accounted for in D_{out} by the spurious root at $\lambda = 0$ introduced by recoordination to “good unknown”. \square

5.6. Stability for small v_0 . Finally, we treat the remaining, “corner case” as v_+ , v_0 simultaneously approach zero. The fact (Lemma 3.5) that

$$\lim_{v_0 \rightarrow 0} \lim_{v_+ \rightarrow 0} D_{\text{in}}(\lambda) \equiv 0$$

shows that this limit is quite delicate; indeed, this is the most delicate part of our analysis.

Proof of Theorem 3.4: inflow case. Consider again the adjoint system

$$\tilde{W}' = -A^*(x, \lambda)\tilde{W}, \quad A^*(x, \lambda) \doteq \begin{pmatrix} 0 & 0 & \hat{v} \\ \bar{\lambda} & 0 & \hat{v} \\ \bar{\lambda} & \bar{\lambda} & f(\hat{v}) - \bar{\lambda} \end{pmatrix}.$$

By the boundary analysis of Section 5.1,

$$\tilde{W} = \left(\alpha, 1, \frac{\alpha \tilde{\mu} - \bar{\lambda}(\alpha + 1)}{-f(\hat{v}) + \bar{\lambda}} \right)^T + O(e^{-\eta|x-\delta|}),$$

where $\alpha := \frac{\tilde{\mu}_+}{\tilde{\mu}_+ + \bar{\lambda}}$, and $\tilde{\mu}$ is the unique stable eigenvalue of A_+^* , satisfying (by matrix perturbation calculation)

$$\tilde{\mu} = \bar{\lambda}(v_+^{1/2} + O(v_+))$$

and thus $\alpha = v_+^{1/2} + O(v_+)$ as $v_0 \rightarrow 0$ (hence $v_+ \rightarrow 0$) on bounded subsets of $\Re \lambda \geq 0$. Combining these expansions, we have

$$\tilde{W}_1(+\infty) = v_+^{1/2}(1 + o(1)), \quad \tilde{W}_3 = \frac{-\bar{\lambda}}{-f(\hat{v}) + \bar{\lambda}}(1 + o(1))$$

for v_0 sufficiently small.

From the \tilde{W}_1 equation $\tilde{W}' = \hat{v}\tilde{W}_3$, we thus obtain

$$\begin{aligned} \tilde{W}_1(0) &= \tilde{W}_1(+\infty) - \int_0^{+\infty} \hat{v}\tilde{W}_3(y) dy \\ &= (1 + o(1)) \times \left(v_+^{1/2} + \int_0^{+\infty} \frac{\bar{\lambda}\hat{v}}{-f(\hat{v}) + \bar{\lambda}}(y) dy \right). \end{aligned}$$

Observing, finally, that, for $\Re \lambda \geq 0$, the ratio of real to imaginary parts of $\frac{\bar{\lambda}\hat{v}}{-f(\hat{v}) + \bar{\lambda}}(y)$ is uniformly positive, we find that $\Re \tilde{W}_1(0) \neq 0$ for v_0 sufficiently small, which yields nonvanishing of $D_{\text{in}}(\lambda)$ on $\Re \lambda \geq 0$ as claimed. \square

6. NUMERICAL COMPUTATIONS

In this section, we show, through a systematic numerical Evans function study, that there are no unstable eigenvalues for

$$(\gamma, v_+) \in [1, 3] \times (0, 1],$$

in either inflow or outflow cases. As defined in Section 2.6, the Evans function is analytic in the right-half plane and reports a value of zero precisely at the eigenvalues of the linearized operator (20). Hence we can use the argument principle to determine if there are any unstable eigenvalues for

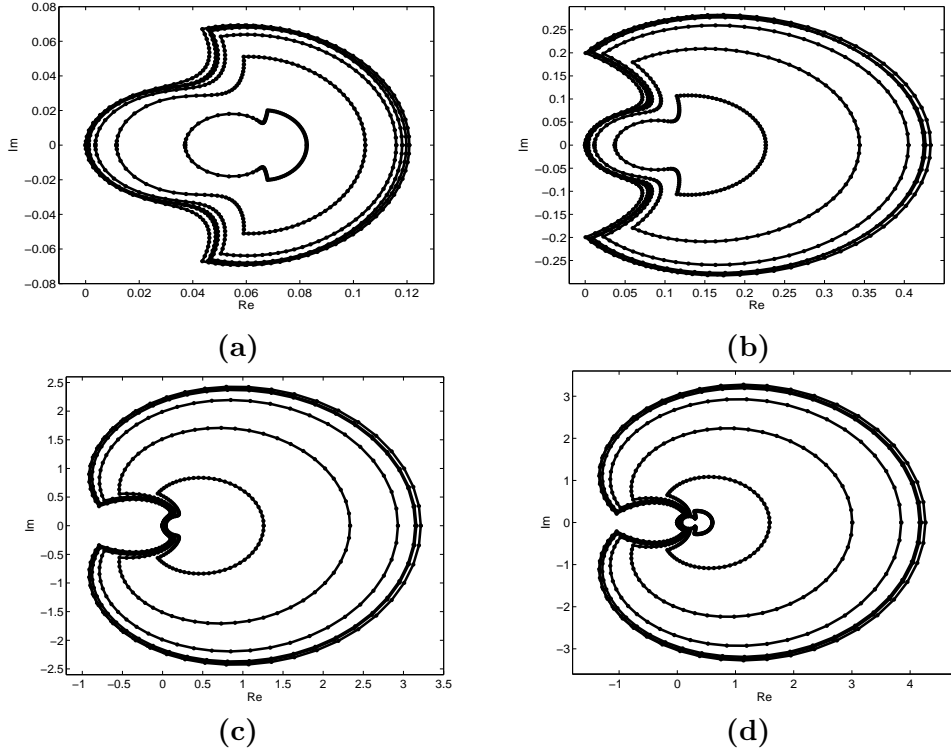


FIGURE 1. Typical examples of the inflow case, showing convergence to the limiting Evans function as $v_+ \rightarrow 0$ for a monatomic gas, $\gamma = 5/3$, with (a) $v_0 = 0.1$, (b) $v_0 = 0.2$, (c) $v_0 = 0.4$, and (d) $v_0 = 0.7$. The contours depicted, going from inner to outer, are images of the semicircle ϕ under D for $v_+ = 1e-2, 1e-3, 1e-4, 1e-5, 1e-6$, with the outer-most contour given by the image of ϕ under D^0 , that is, when $v_+ = 0$. Each contour consists of 60 points in λ .

this system. Our approach closely follows that of [3, 12] for the shock case with only two major differences. First, our shooting algorithm is only one sided as we have the boundary conditions (41) and (47) for the inflow and outflow cases, respectively. Second, we “correct” for the displacement in the boundary layer when $v_0 \approx 1$ in the inflow case and $v_0 \approx 0$ in the outflow case so that the Evans function converges to the shock case as studied in [3, 12] (see discussion in Section 6.3).

The profiles were generated using Matlab’s `bvp4c` routine, which is an adaptive Lobatto quadrature scheme. The shooting portion of the Evans function computation was performed using Matlab’s `ode45` package, which is the standard 4th order adaptive Runge-Kutta-Fehlberg method (RKF45). The error tolerances for both the profiles and the shooting were set to

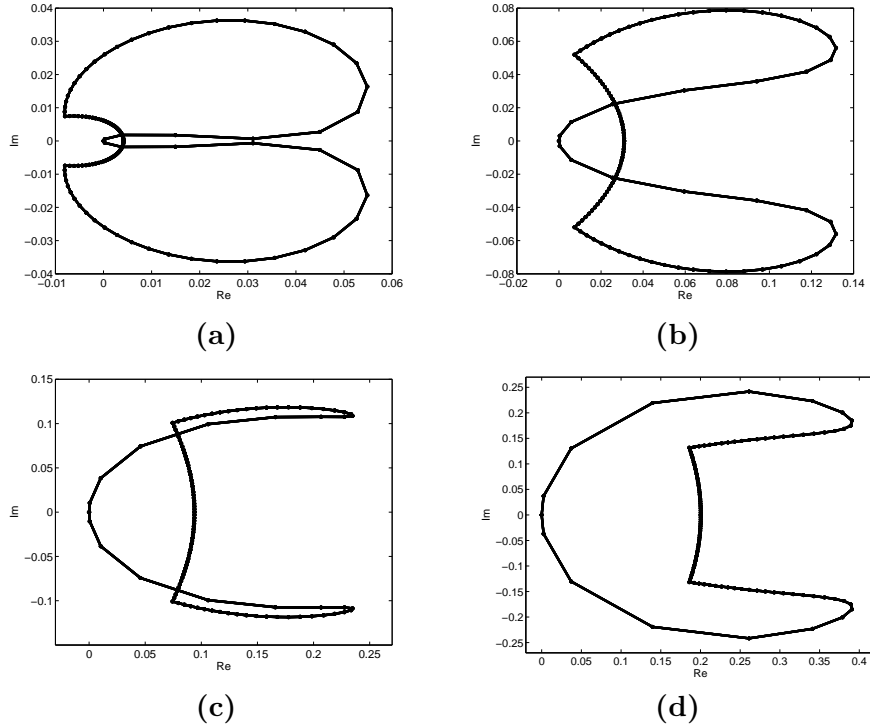


FIGURE 2. Typical examples of the outflow case, showing convergence to the limiting Evans function as $v_+ \rightarrow 0$ for a monatomic gas, $\gamma = 5/3$, with (a) $v_0 = 0.2$, (b) $v_0 = 0.4$, (c) $v_0 = 0.6$, and (d) $v_0 = 0.8$. The contours depicted are images of the semicircle ϕ under D for $v_+ = 1e-2, 1e-3, 1e-4, 1e-5, 1e-6$, and the limiting case $v_+ = 0$. Interestingly the contours are essentially (visually) indistinguishable in this parameter range. Each contour consists of 60 points in λ

AbsTol=1e-6 and **RelTol=1e-8**. We remark that Kato's ODE (see Section 2.6 and [15, 13] for details) is used to analytically choose the initial eigenbasis for the stable/unstable manifolds at the numerical values of infinity at $L = \pm 18$. Finally in Section 6.4, we carry out a numerical convergence study similar to that in [3].

6.1. Winding number computations. The high-frequency estimates in Proposition 2.3 restrict the set of admissible unstable eigenvalues to a fixed compact triangle Λ in the right-half plane (see (31) and (32) for the inflow and outflow cases, respectively). We reiterate the remarkable property that Λ does not depend on the choice of v_+ or v_0 . Hence, to demonstrate stability for a given γ , v_+ and v_0 , it suffices to show that the winding number of the Evans function along a contour containing Λ is zero. Note that in our region

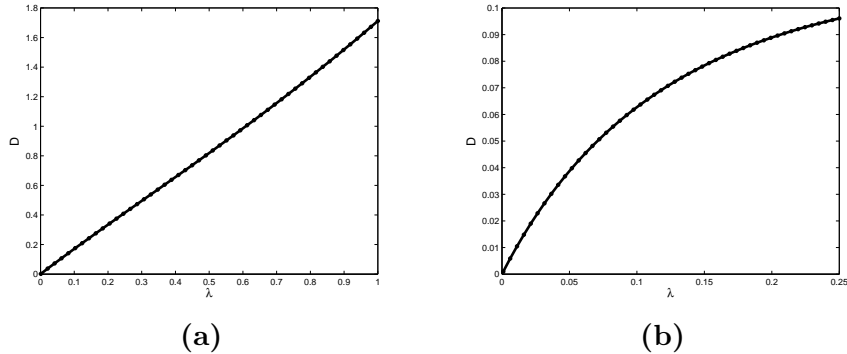


FIGURE 3. Typical examples of the Evans function evaluated along the positive real axis. The (a) inflow case is computed for $v_0 = 0.7$ and $v_+ = 0$ and (b) the outflow case is computed for $v_0 = 0.3$ and $v_+ = 0.001$. Note the transversality at the origin in both cases. Both graphs consist of 50 points in λ .

of interest, $\gamma \in [1, 3]$, the semi-circular contour given by

$$\phi := \partial(\{\lambda \mid \Re \lambda \geq 0\} \cup \{\lambda \mid |\lambda| \leq 10\}),$$

contains Λ in both the inflow and outflow cases. Hence, for consistency we use this same semicircle for all of our winding number computations.

A remarkable feature of the Evans function for this system, and one that is shared with the shock case in [3, 12], is that the Evans function has limiting behavior as the amplitude increases, Section 3.2. For the inflow case, we see in Figure 1, the mapping of the contour ϕ for the monotonic case ($\gamma = 5/3$), for several different choices of v_0 , as $v_+ \rightarrow 0$. We remark that the winding numbers for $0 \leq v_+ \leq 1$ are all zero, and the limiting contour touches zero due to the emergence of a zero root in the limit. Note that the limiting case contains the contours of all other amplitudes. Hence, we have spectral stability for all amplitudes.

The outflow case likewise has a limiting behavior, however, all contours cross through zero due to the eigenvalue at the origin. Nonetheless, since the contours only wind around once, we can likewise conclude that these profiles are spectrally stable. We remark that the outflow case converges to the limiting case faster than the inflow case as is clear from Figure 2. Indeed, $v_+ = 1e-2$ and the limiting case $v_+ = 0$, as well as all of the values of v_+ in between, are virtually indistinguishable.

In our study, we systematically varied v_0 in the interval $[.01, .99]$ and took the $v_+ \rightarrow 0$ limit at each step, starting from a $v_+ = .9$ (or some other appropriate value, for example when $v_0 < .9$) on the small-amplitude end and decreased v_+ steadily to 10^{-k} for $k = 1, 2, 3, \dots, 6$, followed by evaluation at $v_+ = 0$. For both inflow and outflow cases, over 2000 contours were computed. We remark that in the $v_+ \rightarrow 0$ limit, the system becomes

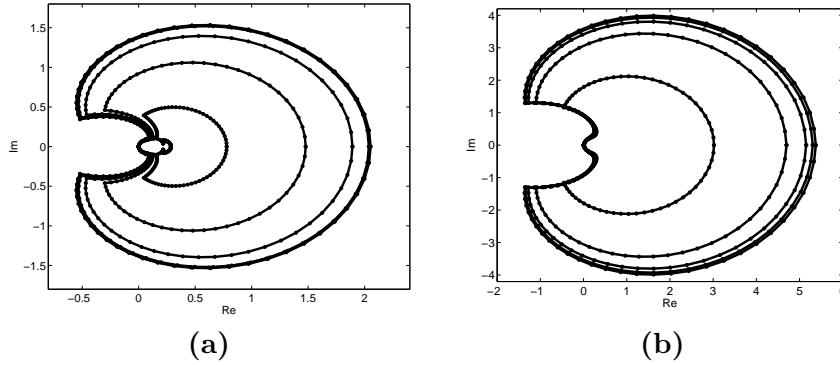


FIGURE 4. Shock limit for (a) inflow and (b) outflow cases, both for $\gamma = 5/3$. Note that the images look very similar to those of [3, 12].

pressureless, and thus all of the contours in the large-amplitude limit look the same regardless of the value of γ chosen.

6.2. Nonexistence of unstable real eigenvalues. As an additional verification of stability, we computed the Evans function along the unstable real axis on the interval $[0, 15]$ for varying parameters to show that there are no real unstable eigenvalues. Since the Evans function has a root at the origin in the limiting system for the inflow case, and for all values of v_+ in the outflow case, we can perform in these cases a sort of *numerical stability index analysis* to verify that the Evans function cuts transversally through the origin and is otherwise nonzero, indicating that there are no unstable real eigenvalues as expected. In Figure 3, we see a typical example of (a) the inflow and (b) outflow cases. Note that in both images, the Evans function cuts transversally through the origin and is otherwise nonzero as λ increases.

6.3. The shock limit. When v_0 is far from the midpoint $(1 - v_+)/2$ of the end states, the the Evans function of the boundary layer is similar to the Evans function of the shock case evaluated at the displacement point x_0 . Hence, when we compute the boundary layer Evans function near the shock limits, $v_0 \approx 1$ for the inflow case and $v_0 \approx 0$ for the outflow case, we multiply for the correction factor $c(\lambda)$ so that our output looks close to that of the shock case studied in [3, 12]. The correction factors are

$$c(\lambda) = e^{(-\mu^+ - \bar{\mu}^-)x_0}$$

for the inflow case and

$$c(\lambda) = e^{(-\bar{\mu}^+ - \mu^-)x_0},$$

for the outflow case, where μ^- is the growth mode of $A_-(\lambda)$ and μ^+ is the decay mode of $A_+(\lambda)$. In Figure 4, we see that these highly displaced profiles

Inflow Case						
L	$\gamma = 1.2$	$\gamma = 1.4$	$\gamma = 1.666$	$\gamma = 2.0$	$\gamma = 2.5$	$\gamma = 3.0$
8	7.8(-1)	8.4(-1)	9.2(-1)	1.0(0)	1.2(0)	1.3(0)
10	1.4(-1)	1.2(-1)	9.2(-2)	6.8(-2)	4.4(-2)	2.8(-2)
12	1.4(-2)	7.9(-3)	3.6(-3)	1.3(-3)	3.1(-4)	7.3(-5)
14	1.3(-3)	4.9(-4)	1.3(-4)	2.4(-5)	8.7(-6)	8.2(-6)
16	1.2(-4)	3.0(-5)	4.7(-6)	2.8(-6)	2.7(-6)	2.6(-6)
18	1.1(-5)	5.8(-6)	8.0(-6)	8.1(-6)	8.0(-6)	8.0(-6)
Outflow Case						
L	$\gamma = 1.2$	$\gamma = 1.4$	$\gamma = 1.666$	$\gamma = 2.0$	$\gamma = 2.5$	$\gamma = 3.0$
8	5.4(-3)	5.4(-3)	5.4(-3)	5.4(-3)	5.4(-3)	5.4(-3)
10	9.2(-4)	9.1(-4)	9.1(-4)	9.1(-4)	9.1(-4)	9.1(-4)
12	1.5(-4)	1.5(-4)	1.5(-4)	1.5(-4)	1.5(-4)	1.5(-4)
14	2.5(-5)	2.7(-5)	2.0(-5)	2.0(-5)	2.0(-5)	2.0(-5)
16	2.3(-6)	2.6(-6)	2.6(-6)	2.5(-6)	2.5(-6)	2.5(-6)
18	6.6(-6)	3.6(-6)	8.7(-6)	8.7(-6)	8.7(-6)	8.7(-6)

TABLE 1. Relative errors in $D(\lambda)$ for the inflow and outflow cases are computed by taking the maximum relative error for 60 contour points evaluated along the semicircle ϕ . Samples were taken for varying L and γ , leaving v_+ fixed at $v_+ = 10^{-4}$ and $v_0 = 0.6$. We used $L = 8, 10, 12, 14, 16, 18, 20$ and $\gamma = 1.2, 1.4, 1.666, 2.0$. Relative errors were computed using the next value of L as the baseline.

appear to be very similar to the shock cases with one notable difference. These images have a small dimple near $\lambda = 0$ to account for the eigenvalue there, whereas those in the shock case [3, 12] were computed in integrated coordinates and thus have no root at the origin.

6.4. Numerical convergence study. As in [3], we carry out a numerical convergence study to show that our results are accurate. We varied the absolute and relative error tolerances, as well as the length of the numerical domain $[-L, L]$. In Tables 1–2, we demonstrate that our choices of $L = 18$, $\text{AbsTol} = 1\text{e-}6$ and $\text{RelTol} = 1\text{e-}8$ provide accurate results.

APPENDIX A. PROOF OF PRELIMINARY ESTIMATE: INFLOW CASE

Our starting point is Remark 2.4, in which we observed that the first-order eigensystem (34) in variable $W = (w, u - v, v)^T$ may be converted by the rescaling $W \rightarrow \tilde{W} := (w, u - v, \lambda v)^T$ to a system identical to that of the integrated equations in the shock case; see [22]. Artificially defining

Inflow Case						
Abs/Rel	$\gamma = 1.2$	$\gamma = 1.4$	$\gamma = 1.666$	$\gamma = 2.0$	$\gamma = 2.5$	$\gamma = 3.0$
$10^{-3}/10^{-5}$	5.4(-4)	4.1(-4)	4.0(-4)	5.0(-4)	3.4(-4)	8.6(-4)
$10^{-4}/10^{-6}$	3.1(-5)	4.6(-5)	3.4(-5)	3.3(-5)	3.3(-5)	3.2(-5)
$10^{-5}/10^{-7}$	2.9(-6)	3.6(-6)	3.9(-6)	6.8(-6)	2.7(-6)	2.5(-6)
$10^{-6}/10^{-8}$	4.6(-7)	9.9(-7)	1.1(-6)	6.0(-7)	2.9(-7)	3.2(-7)
Outflow Case						
Abs/Rel	$\gamma = 1.2$	$\gamma = 1.4$	$\gamma = 1.666$	$\gamma = 2.0$	$\gamma = 2.5$	$\gamma = 3.0$
$10^{-3}/10^{-5}$	9.2(-4)	9.2(-4)	9.1(-4)	9.1(-4)	9.1(-4)	9.2(-4)
$10^{-4}/10^{-6}$	5.3(-5)	4.9(-5)	5.3(-5)	5.3(-5)	5.3(-5)	5.3(-5)
$10^{-5}/10^{-7}$	6.7(-5)	6.7(-5)	6.7(-5)	6.7(-5)	6.7(-5)	6.7(-5)
$10^{-6}/10^{-8}$	2.9(-6)	2.9(-6)	2.9(-6)	2.9(-6)	2.9(-6)	2.9(-6)

TABLE 2. Relative errors in $D(\lambda)$ for the inflow and outflow cases are computed by taking the maximum relative error for 60 contour points evaluated along the semicircle ϕ . Samples were taken for varying the absolute and relative error tolerances and γ in the ODE solver, leaving $L = 18$ and $\gamma = 1.666$, $v_+ = 10^{-4}$, and $v_0 = 0.6$ fixed. Relative errors were computed using the next run as the baseline.

$(\tilde{u}, \tilde{v}, \tilde{v}')^T := \tilde{W}$, we obtain a system

$$(94a) \quad \lambda \tilde{v} + \tilde{v}' - \tilde{u}' = 0,$$

$$(94b) \quad \lambda \tilde{u} + \tilde{u}' - \frac{h(\hat{v})}{\hat{v}^{\gamma+1}} \tilde{v}' = \frac{\tilde{u}''}{\hat{v}}.$$

identical to that in the integrated shock case [3], but with boundary conditions

$$(95) \quad \tilde{v}(0) = \tilde{v}'(0) = \tilde{u}'(0) = 0$$

imposed at $x = 0$. This new eigenvalue problem differs spectrally from (22) only at $\lambda = 0$, hence spectral stability of (22) is implied by spectral stability of (94). Hereafter, we drop the tildes, and refer simply to u, v .

With these coordinates, we may establish (2.3) by exactly the same argument used in the shock case in [3, 12], for completeness reproduced here.

Lemma A.1. *The following identity holds for $\Re\lambda \geq 0$:*

$$(96) \quad \begin{aligned} (\Re(\lambda) + |\Im(\lambda)|) \int_{\mathbb{R}^+} \hat{v}|u|^2 + \int_{\mathbb{R}^+} |u'|^2 \\ \leq \sqrt{2} \int_{\mathbb{R}^+} \frac{h(\hat{v})}{\hat{v}^\gamma} |v'| |u| + \sqrt{2} \int_{\mathbb{R}^+} \hat{v} |u'| |u|. \end{aligned}$$

Proof. We multiply (94b) by $\hat{v}\bar{u}$ and integrate along x . This yields

$$\lambda \int_{\mathbb{R}^+} \hat{v}|u|^2 + \int_{\mathbb{R}^+} \hat{v}u'\bar{u} + \int_{\mathbb{R}^+} |u'|^2 = \int_{\mathbb{R}^+} \frac{h(\hat{v})}{\hat{v}^\gamma} v'\bar{u}.$$

We get (96) by taking the real and imaginary parts and adding them together, and noting that $|\Re(z)| + |\Im(z)| \leq \sqrt{2}|z|$. \square

Lemma A.2. *The following identity holds for $\Re\lambda \geq 0$:*

$$(97) \quad \int_{\mathbb{R}^+} |u'|^2 = 2\Re(\lambda)^2 \int_{\mathbb{R}^+} |v|^2 + \Re(\lambda) \int_{\mathbb{R}^+} \frac{|v'|^2}{\hat{v}} + \frac{1}{2} \int_{\mathbb{R}^+} \left[\frac{h(\hat{v})}{\hat{v}^{\gamma+1}} + \frac{a\gamma}{\hat{v}^{\gamma+1}} \right] |v'|^2$$

Proof. We multiply (94b) by \bar{v}' and integrate along x . This yields

$$\lambda \int_{\mathbb{R}^+} u\bar{v}' + \int_{\mathbb{R}^+} u'\bar{v}' - \int_{\mathbb{R}^+} \frac{h(\hat{v})}{\hat{v}^{\gamma+1}} |v'|^2 = \int_{\mathbb{R}^+} \frac{1}{\hat{v}} u''\bar{v}' = \int_{\mathbb{R}^+} \frac{1}{\hat{v}} (\lambda v' + v'')\bar{v}'.$$

Using (94a) on the right-hand side, integrating by parts, and taking the real part gives

$$\Re \left[\lambda \int_{\mathbb{R}^+} u\bar{v}' + \int_{\mathbb{R}^+} u'\bar{v}' \right] = \int_{\mathbb{R}^+} \left[\frac{h(\hat{v})}{\hat{v}^{\gamma+1}} + \frac{\hat{v}_x}{2\hat{v}^2} \right] |v'|^2 + \Re(\lambda) \int_{\mathbb{R}^+} \frac{|v'|^2}{\hat{v}}.$$

The right hand side can be rewritten as

$$(98) \quad \Re \left[\lambda \int_{\mathbb{R}^+} u\bar{v}' + \int_{\mathbb{R}^+} u'\bar{v}' \right] = \frac{1}{2} \int_{\mathbb{R}^+} \left[\frac{h(\hat{v})}{\hat{v}^{\gamma+1}} + \frac{a\gamma}{\hat{v}^{\gamma+1}} \right] |v'|^2 + \Re(\lambda) \int_{\mathbb{R}^+} \frac{|v'|^2}{\hat{v}}.$$

Now we manipulate the left-hand side. Note that

$$\begin{aligned} \lambda \int_{\mathbb{R}^+} u\bar{v}' + \int_{\mathbb{R}^+} u'\bar{v}' &= (\lambda + \bar{\lambda}) \int_{\mathbb{R}^+} u\bar{v}' - \int_{\mathbb{R}^+} u(\bar{\lambda}\bar{v}' + \bar{v}'') \\ &= -2\Re(\lambda) \int_{\mathbb{R}^+} u'\bar{v} - \int_{\mathbb{R}^+} u\bar{u}'' \\ &= -2\Re(\lambda) \int_{\mathbb{R}^+} (\lambda v + v')\bar{v} + \int_{\mathbb{R}^+} |u'|^2. \end{aligned}$$

Hence, by taking the real part we get

$$\Re \left[\lambda \int_{\mathbb{R}^+} u\bar{v}' + \int_{\mathbb{R}^+} u'\bar{v}' \right] = \int_{\mathbb{R}^+} |u'|^2 - 2\Re(\lambda)^2 \int_{\mathbb{R}^+} |v|^2.$$

This combines with (98) to give (97). \square

Lemma A.3 ([3]). *For $h(\hat{v})$ as in (21), we have*

$$(99) \quad \sup_{\hat{v}} \left| \frac{h(\hat{v})}{\hat{v}^\gamma} \right| = \gamma \frac{1 - v_+}{1 - v_+^\gamma} \leq \gamma,$$

where \hat{v} is the profile solution to (18).

Proof. Defining

$$(100) \quad g(\hat{v}) := h(\hat{v})\hat{v}^{-\gamma} = -\hat{v} + a(\gamma - 1)\hat{v}^{-\gamma} + (a + 1),$$

we have $g'(\hat{v}) = -1 - a\gamma(\gamma - 1)\hat{v}^{-\gamma-1} < 0$ for $0 < v_+ \leq \hat{v} \leq v_- = 1$, hence the maximum of g on $\hat{v} \in [v_+, v_-]$ is achieved at $\hat{v} = v_+$. Substituting (19) into (100) and simplifying yields (99). \square

Proof of Proposition 2.3. Using Young's inequality twice on right-hand side of (96) together with (99), we get

$$\begin{aligned}
& (\Re e(\lambda) + |\Im m(\lambda)|) \int_{\mathbb{R}^+} \hat{v}|u|^2 + \int_{\mathbb{R}^+} |u'|^2 \\
& \leq \sqrt{2} \int_{\mathbb{R}^+} \frac{h(\hat{v})}{\hat{v}^\gamma} |v'| |u| + \sqrt{2} \int_{\mathbb{R}^+} \hat{v} |u'| |u| \\
& \leq \theta \int_{\mathbb{R}^+} \frac{h(\hat{v})}{\hat{v}^{\gamma+1}} |v'|^2 + \frac{(\sqrt{2})^2}{4\theta} \int_{\mathbb{R}^+} \frac{h(\hat{v})}{\hat{v}^\gamma} \hat{v} |u|^2 + \epsilon \int_{\mathbb{R}^+} \hat{v} |u'|^2 + \frac{1}{4\epsilon} \int_{\mathbb{R}^+} \hat{v} |u|^2 \\
& < \theta \int_{\mathbb{R}^+} \frac{h(\hat{v})}{\hat{v}^{\gamma+1}} |v'|^2 + \epsilon \int_{\mathbb{R}^+} |u'|^2 + \left[\frac{\gamma}{2\theta} + \frac{1}{2\epsilon} \right] \int_{\mathbb{R}^+} \hat{v} |u|^2.
\end{aligned}$$

Assuming that $0 < \epsilon < 1$ and $\theta = (1 - \epsilon)/2$, this simplifies to

$$\begin{aligned}
& (\Re e(\lambda) + |\Im m(\lambda)|) \int_{\mathbb{R}^+} \hat{v}|u|^2 + (1 - \epsilon) \int_{\mathbb{R}^+} |u'|^2 \\
& < \frac{1 - \epsilon}{2} \int_{\mathbb{R}^+} \frac{h(\hat{v})}{\hat{v}^{\gamma+1}} |v'|^2 + \left[\frac{\gamma}{2\theta} + \frac{1}{2\epsilon} \right] \int_{\mathbb{R}^+} \hat{v} |u|^2.
\end{aligned}$$

Applying (97) yields

$$(\Re e(\lambda) + |\Im m(\lambda)|) \int_{\mathbb{R}^+} \hat{v}|u|^2 < \left[\frac{\gamma}{1 - \epsilon} + \frac{1}{2\epsilon} \right] \int_{\mathbb{R}^+} \hat{v}|u|^2,$$

or equivalently,

$$(\Re e(\lambda) + |\Im m(\lambda)|) < \frac{(2\gamma - 1)\epsilon + 1}{2\epsilon(1 - \epsilon)}.$$

Setting $\epsilon = 1/(2\sqrt{\gamma} + 1)$ gives (31). \square

APPENDIX B. PROOF OF PRELIMINARY ESTIMATE: OUTFLOW CASE

Similarly as in the inflow case, we can convert the eigenvalue equations into the integrated equations as in the shock case; see [22]. Artificially defining $(\tilde{u}, \tilde{v}, \tilde{v}')^T := \tilde{W}$, we obtain a system

$$(101a) \quad \lambda \tilde{v} + \tilde{v}' - \tilde{u}' = 0,$$

$$(101b) \quad \lambda \tilde{u} + \tilde{u}' - \frac{h(\hat{v})}{\hat{v}^{\gamma+1}} \tilde{v}' = \frac{\tilde{u}''}{\hat{v}}.$$

identical to that in the integrated shock case [3], but with boundary conditions

$$(102) \quad \tilde{v}'(0) = \frac{\lambda}{\alpha - 1} \tilde{v}(0), \quad \tilde{u}'(0) = \alpha \tilde{v}'(0)$$

imposed at $x = 0$. We shall write w_0 for $w(0)$, for any function w . This new eigenvalue problem differs spectrally from (22) only at $\lambda = 0$, hence spectral stability of (22) is implied by spectral stability of (101). Hereafter, we drop the tildes, and refer simply to u, v .

Lemma B.1. *The following identity holds for $\Re\lambda \geq 0$:*

$$(103) \quad \begin{aligned} & (\Re(\lambda) + |\Im(\lambda)|) \int_{\mathbb{R}^-} \hat{v}|u|^2 - \frac{1}{2} \int_{\mathbb{R}^-} \hat{v}_x|u|^2 + \int_{\mathbb{R}^-} |u'|^2 + \frac{1}{2} \hat{v}_0|u_0|^2 \\ & \leq \sqrt{2} \int_{\mathbb{R}^-} \frac{h(\hat{v})}{\hat{v}^\gamma} |v'| |u| + \int_{\mathbb{R}^-} \hat{v}|u'| |u| + \sqrt{2} |\alpha| |v'_0| |u_0|. \end{aligned}$$

Proof. We multiply (101b) by $\hat{v}\bar{u}$ and integrate along x . This yields

$$\lambda \int_{\mathbb{R}^-} \hat{v}|u|^2 + \int_{\mathbb{R}^-} \hat{v}u'\bar{u} + \int_{\mathbb{R}^-} |u'|^2 = \int_{\mathbb{R}^-} \frac{h(\hat{v})}{\hat{v}^\gamma} v'\bar{u} + u'_0\bar{u}_0.$$

We get (103) by taking the real and imaginary parts and adding them together, and noting that $|\Re(z)| + |\Im(z)| \leq \sqrt{2}|z|$. \square

Lemma B.2. *The following inequality holds for $\Re\lambda \geq 0$:*

$$(104) \quad \begin{aligned} & \frac{1}{2} \int_{\mathbb{R}^-} \left[\frac{h(\hat{v})}{\hat{v}^{\gamma+1}} + \frac{a\gamma}{\hat{v}^{\gamma+1}} \right] |v'|^2 + \Re(\lambda) \int_{\mathbb{R}^-} \frac{|v'|^2}{\hat{v}} + \frac{|v'_0|^2}{4\hat{v}_0} + 2\Re\lambda^2 \int_{\mathbb{R}^-} |v|^2 \\ & \leq \int_{\mathbb{R}^-} |u'|^2 + \hat{v}_0|u_0|^2. \end{aligned}$$

Proof. We multiply (101b) by \bar{v}' and integrate along x . This yields

$$\lambda \int_{\mathbb{R}^-} u\bar{v}' + \int_{\mathbb{R}^-} u'\bar{v}' - \int_{\mathbb{R}^-} \frac{h(\hat{v})}{\hat{v}^{\gamma+1}} |v'|^2 = \int_{\mathbb{R}^-} \frac{1}{\hat{v}} u''\bar{v}' = \int_{\mathbb{R}^-} \frac{1}{\hat{v}} (\lambda v' + v'')\bar{v}'.$$

Using (101a) on the right-hand side, integrating by parts, and taking the real part gives

$$\Re \left[\lambda \int_{\mathbb{R}^-} u\bar{v}' + \int_{\mathbb{R}^-} u'\bar{v}' \right] = \int_{\mathbb{R}^-} \left[\frac{h(\hat{v})}{\hat{v}^{\gamma+1}} + \frac{\hat{v}_x}{2\hat{v}^2} \right] |v'|^2 + \Re(\lambda) \int_{\mathbb{R}^-} \frac{|v'|^2}{\hat{v}} + \frac{|v'_0|^2}{2\hat{v}_0}.$$

The right hand side can be rewritten as

$$(105) \quad \begin{aligned} & \Re \left[\lambda \int_{\mathbb{R}^-} u\bar{v}' + \int_{\mathbb{R}^-} u'\bar{v}' \right] \\ & = \frac{1}{2} \int_{\mathbb{R}^-} \left[\frac{h(\hat{v})}{\hat{v}^{\gamma+1}} + \frac{a\gamma}{\hat{v}^{\gamma+1}} \right] |v'|^2 + \Re(\lambda) \int_{\mathbb{R}^-} \frac{|v'|^2}{\hat{v}} + \frac{|v'_0|^2}{2\hat{v}_0}. \end{aligned}$$

Now we manipulate the left-hand side. Note that

$$\begin{aligned} \lambda \int_{\mathbb{R}^-} u\bar{v}' + \int_{\mathbb{R}^-} u'\bar{v}' &= (\lambda + \bar{\lambda}) \int_{\mathbb{R}^-} u\bar{v}' + \int_{\mathbb{R}^-} (u'\bar{v}' - \bar{\lambda}u\bar{v}') \\ &= -2\Re(\lambda) \int_{\mathbb{R}^-} u'\bar{v} + 2\Re\lambda u_0\bar{v}_0 + \int_{\mathbb{R}^-} u'(\bar{v}' + \bar{\lambda}\bar{v}) - \bar{\lambda}u_0\bar{v}_0 \\ &= -2\Re(\lambda) \int_{\mathbb{R}^-} (\lambda v + v')\bar{v} + \int_{\mathbb{R}^-} |u'|^2 + 2\Re\lambda u_0\bar{v}_0 - \bar{\lambda}u_0\bar{v}_0. \end{aligned}$$

Hence, by taking the real part and noting that

$$\Re(2\Re\lambda u_0\bar{v}_0 - \bar{\lambda}u_0\bar{v}_0) = \Re\lambda\Re(u_0\bar{v}_0) - \Im\lambda\Im(u_0\bar{v}_0) = \Re(\lambda u_0\bar{v}_0)$$

we get

$$\Re \left[\lambda \int_{\mathbb{R}^-} u \bar{v}' + \int_{\mathbb{R}^-} u' \bar{v}' \right] = \int_{\mathbb{R}^-} |u'|^2 - 2\Re \lambda^2 \int_{\mathbb{R}^-} |v|^2 - \Re \lambda |v_0|^2 + \Re(\lambda u_0 \bar{v}_0).$$

This combines with (105) to give

$$\begin{aligned} \frac{1}{2} \int_{\mathbb{R}^-} \left[\frac{h(\hat{v})}{\hat{v}^{\gamma+1}} + \frac{a\gamma}{\hat{v}^{\gamma+1}} \right] |v'|^2 + \Re(\lambda) \int_{\mathbb{R}^-} \frac{|v'|^2}{\hat{v}} + \frac{|v_0'|^2}{2\hat{v}_0} + 2\Re \lambda^2 \int_{\mathbb{R}^-} |v|^2 \\ + \Re \lambda |v_0|^2 = \int_{\mathbb{R}^-} |u'|^2 + \Re(\lambda u_0 \bar{v}_0). \end{aligned}$$

We get (104) by observing that (102) and Young's inequality yield

$$|\Re(\lambda u_0 \bar{v}_0)| \leq |\alpha - 1| |v_0' v_0| \leq |v_0' v_0| \leq \frac{|v_0'|^2}{4\hat{v}_0} + \hat{v}_0 |u_0|^2.$$

Here we used $|\alpha - 1| = \frac{|\lambda|}{|\lambda - \hat{v}_0'|} \leq 1$. Note that $\Re \lambda \geq 0$ and $\hat{v}_0' \leq 0$. \square

Proof of Proposition 2.3. Using Young's inequality twice on right-hand side of (103) together with (99), and denoting the boundary term on the right by I_b , we get

$$\begin{aligned} (\Re(\lambda) + |\Im(\lambda)|) \int_{\mathbb{R}^-} \hat{v} |u|^2 - \frac{1}{2} \int_{\mathbb{R}^-} \hat{v}_x |u|^2 + \int_{\mathbb{R}^-} |u'|^2 + \frac{1}{2} \hat{v}_0 |u_0|^2 \\ \leq \sqrt{2} \int_{\mathbb{R}^-} \frac{h(\hat{v})}{\hat{v}^\gamma} |v'| |u| + \int_{\mathbb{R}^-} \hat{v} |u'| |u| + I_b \\ \leq \theta \int_{\mathbb{R}^-} \frac{h(\hat{v})}{\hat{v}^{\gamma+1}} |v'|^2 + \frac{1}{2\theta} \int_{\mathbb{R}^-} \frac{h(\hat{v})}{\hat{v}^\gamma} \hat{v} |u|^2 + \epsilon \int_{\mathbb{R}^-} \hat{v} |u'|^2 + \frac{1}{4\epsilon} \int_{\mathbb{R}^-} \hat{v} |u|^2 + I_b \\ < \theta \int_{\mathbb{R}^-} \frac{h(\hat{v})}{\hat{v}^{\gamma+1}} |v'|^2 + \epsilon \int_{\mathbb{R}^-} |u'|^2 + \left[\frac{\gamma}{2\theta} + \frac{1}{4\epsilon} \right] \int_{\mathbb{R}^-} \hat{v} |u|^2 + I_b. \end{aligned}$$

Here we treat the boundary term by

$$I_b \leq \sqrt{2} |\alpha| |v_0'| |u_0| \leq \frac{\theta |v_0'|^2}{2\hat{v}_0} + \frac{1}{\theta} |\alpha|^2 \hat{v}_0 |u_0|^2.$$

Therefore using (104), we simply obtain from the above estimates

$$\begin{aligned} (\Re(\lambda) + |\Im(\lambda)|) \int_{\mathbb{R}^-} \hat{v} |u|^2 + (1 - \epsilon) \int_{\mathbb{R}^-} |u'|^2 + \frac{1}{2} \hat{v}_0 |u_0|^2 \\ < \theta \int_{\mathbb{R}^-} \frac{h(\hat{v})}{\hat{v}^{\gamma+1}} |v'|^2 + \frac{\theta |v_0'|^2}{2\hat{v}_0} + \left[\frac{\gamma}{2\theta} + \frac{1}{4\epsilon} \right] \int_{\mathbb{R}^-} \hat{v} |u|^2 + \frac{1}{\theta} |\alpha|^2 \hat{v}_0 |u_0|^2 \\ < 2\theta \int_{\mathbb{R}^-} |u'|^2 + \left[\frac{\gamma}{2\theta} + \frac{1}{4\epsilon} \right] \int_{\mathbb{R}^-} \hat{v} |u|^2 + J_b \end{aligned}$$

where $J_b := (\frac{1}{\theta} |\alpha|^2 + 2\theta) \hat{v}_0 |u_0|^2$. Assuming that $\epsilon + 2\theta \leq 1$, this simplifies to

$$(\Re(\lambda) + |\Im(\lambda)|) \int_{\mathbb{R}^-} \hat{v} |u|^2 + \frac{1}{2} \hat{v}_0 |u_0|^2 < \left[\frac{\gamma}{2\theta} + \frac{1}{4\epsilon} \right] \int_{\mathbb{R}^-} \hat{v} |u|^2 + J_b.$$

Note that $|\alpha| \leq \frac{-\hat{v}'_0}{|\lambda|} \leq \frac{1}{4|\lambda|}$. Therefore for $|\lambda| \geq \frac{1}{4\theta}$, we get $|\alpha| \leq \theta$ and $J_b \leq 3\theta\hat{v}_0|u_0|^2$. For sake of simplicity, choose $\theta = 1/6$ and $\epsilon = 2/3$. This shows that J_b can be absorbed into the left by the term $\frac{1}{2}\hat{v}_0|u_0|^2$ and thus we get

$$(\Re e(\lambda) + |\Im m(\lambda)|) \int_{\mathbb{R}^-} \hat{v}|u|^2 < \left[\frac{\gamma}{2\theta} + \frac{1}{4\epsilon} \right] \int_{\mathbb{R}^-} \hat{v}|u|^2 = \left[3\gamma + \frac{3}{8} \right] \int_{\mathbb{R}^-} \hat{v}|u|^2,$$

provided that $|\lambda| \geq 1/(4\theta) = 3/2$.

This shows

$$(\Re e(\lambda) + |\Im m(\lambda)|) < \max\left\{ \frac{3\sqrt{2}}{2}, 3\gamma + \frac{3}{8} \right\}.$$

□

APPENDIX C. NONVANISHING OF D_{in}^0

Working in (\tilde{v}, \tilde{u}) variables as in (94), the limiting eigenvalue system and boundary conditions take the form

$$(106a) \quad \lambda\tilde{v} + \tilde{v}' - \tilde{u}' = 0,$$

$$(106b) \quad \lambda\tilde{u} + \tilde{u}' - \frac{1 - \hat{v}}{\hat{v}}\tilde{v}' = \frac{\tilde{u}''}{\hat{v}}.$$

corresponding to a pressureless gas, $\gamma = 0$, with

$$(107) \quad (\tilde{u}, \tilde{u}', \tilde{v}, \tilde{v}')(0) = (d, 0, 0, 0), \quad (\tilde{u}, \tilde{u}', \tilde{v}, \tilde{v}')(+\infty) = (c, 0, 0, 0).$$

Hereafter, we drop the tildes.

Proof of Proposition 3.6. Multiplying (106b) by $\hat{v}\bar{u}/(1 - \hat{v})$ and integrating on $[0, b] \subset \mathbb{R}^+$, we obtain

$$\lambda \int_0^b \frac{\hat{v}}{1 - \hat{v}} |u|^2 dx + \int_0^b \frac{\hat{v}}{1 - \hat{v}} u' \bar{u} dx - \int_0^b v' \bar{u} dx = \int_0^b \frac{u'' \bar{u}}{1 - \hat{v}} dx.$$

Integrating the third and fourth terms by parts yields

$$\begin{aligned} & \lambda \int_0^b \frac{\hat{v}}{1 - \hat{v}} |u|^2 dx + \int_0^b \left[\frac{\hat{v}}{1 - \hat{v}} + \left(\frac{1}{1 - \hat{v}} \right)' \right] u' \bar{u} dx \\ & \quad + \int_0^b \frac{|u'|^2}{1 - \hat{v}} dx + \int_0^b v(\overline{\lambda v + v'}) dx \\ & = \left[v\bar{u} + \frac{u'\bar{u}}{1 - \hat{v}} \right] \Big|_0^b. \end{aligned}$$

Taking the real part, we have

$$\begin{aligned}
& \Re e(\lambda) \int_0^b \left(\frac{\hat{v}}{1-\hat{v}} |u|^2 + |v|^2 \right) dx + \int_0^b g(\hat{v}) |u|^2 dx + \int_0^b \frac{|u'|^2}{1-\hat{v}} dx \\
(108) \quad & = \Re e \left[v\bar{u} + \frac{u'\bar{u}}{1-\hat{v}} - \frac{1}{2} \left[\frac{\hat{v}}{1-\hat{v}} + \left(\frac{1}{1-\hat{v}} \right)' \right] |u|^2 - \frac{|v|^2}{2} \right] \Big|_0^b,
\end{aligned}$$

where

$$g(\hat{v}) = -\frac{1}{2} \left[\left(\frac{\hat{v}}{1-\hat{v}} \right)' + \left(\frac{1}{1-\hat{v}} \right)'' \right].$$

Note that

$$\frac{d}{dx} \left(\frac{1}{1-\hat{v}} \right) = -\frac{(1-\hat{v})'}{(1-\hat{v})^2} = \frac{\hat{v}_x}{(1-\hat{v})^2} = \frac{\hat{v}(\hat{v}-1)}{(1-\hat{v})^2} = -\frac{\hat{v}}{1-\hat{v}}.$$

Thus, $g(\hat{v}) \equiv 0$ and the third term on the right-hand side vanishes, leaving

$$\begin{aligned}
& \Re e(\lambda) \int_0^b \left(\frac{\hat{v}}{1-\hat{v}} |u|^2 + |v|^2 \right) dx + \int_0^b \frac{|u'|^2}{1-\hat{v}} dx \\
& = \left[\Re e(v\bar{u}) + \frac{\Re e(u'\bar{u})}{1-\hat{v}} - \frac{|v|^2}{2} \right] \Big|_0^b \\
& = \left[\Re e(v\bar{u}) + \frac{\Re e(u'\bar{u})}{1-\hat{v}} - \frac{|v|^2}{2} \right] (b).
\end{aligned}$$

We show finally that the right-hand side goes to zero in the limit as $b \rightarrow \infty$. By Proposition 4.3, the behavior of u, v near $\pm\infty$ is governed by the limiting constant-coefficient systems $W' = A_{\pm}^0(\lambda)W$, where $W = (u, v, v')^T$ and $A_{\pm}^0 = A^0(\pm\infty, \lambda)$. In particular, solutions W asymptotic to $(1, 0, 0)$ at $x = +\infty$ decay exponentially in (u', v, v') and are bounded in coordinate u as $x \rightarrow +\infty$. Observing that $1-\hat{v} \rightarrow 1$ as $x \rightarrow +\infty$, we thus see immediately that the boundary contribution at b vanishes as $b \rightarrow +\infty$.

Thus, in the limit as $b \rightarrow +\infty$,

$$(109) \quad \Re e(\lambda) \int_0^{+\infty} \left(\frac{\hat{v}}{1-\hat{v}} |u|^2 + |v|^2 \right) dx + \int_0^{+\infty} \frac{|u'|^2}{1-\hat{v}} dx = 0.$$

But, for $\Re e\lambda \geq 0$, this implies $u' \equiv 0$, or $u \equiv \text{constant}$, which, by $u(0) = 1$, implies $u \equiv 1$. This reduces (106a) to $v' = \lambda v$, yielding the explicit solution $v = Ce^{\lambda x}$. By $v(0) = 0$, therefore, $v \equiv 0$ for $\Re e\lambda \geq 0$. Substituting into (106b), we obtain $\lambda = 0$. It follows that there are no nontrivial solutions of (106), (107) for $\Re e\lambda \geq 0$ except at $\lambda = 0$. \square

Remark C.1. *The above energy estimate is essentially identical to that used in [12] to treat the limiting shock case.*

APPENDIX D. NONVANISHING OF D_{out}^0

Working in (\tilde{v}, \tilde{u}) variables as in (94), the limiting eigenvalue system and boundary conditions take the form

$$(110a) \quad \lambda \tilde{v} + \tilde{v}' - \tilde{u}' = 0,$$

$$(110b) \quad \lambda \tilde{u} + \tilde{u}' - \frac{1 - \hat{v}}{\hat{v}} \tilde{v}' = \frac{\tilde{u}''}{\hat{v}}.$$

corresponding to a pressureless gas, $\gamma = 0$, with

$$(111) \quad (\tilde{u}, \tilde{u}', \tilde{v}, \tilde{v}')(-\infty) = (0, 0, 0, 0),$$

$$(112) \quad \tilde{v}'(0) = \frac{\lambda}{\alpha - 1} \tilde{v}(0), \quad \tilde{u}'(0) = \alpha \tilde{v}'(0).$$

In particular,

$$(113) \quad \tilde{u}'(0) = \frac{\lambda \alpha}{\alpha - 1} \tilde{v}(0) = \hat{v}'(0) \tilde{v}(0) = (v_0 - 1) \hat{v}_0 \tilde{v}(0).$$

Hereafter, we drop the tildes.

Proof of Proposition 3.6. Multiplying (110b) by $\hat{v}\bar{u}/(1 - \hat{v})$ and integrating on $[a, 0] \subset \mathbb{R}^-$, we obtain

$$\lambda \int_a^0 \frac{\hat{v}}{1 - \hat{v}} |u|^2 dx + \int_a^b \frac{\hat{v}}{1 - \hat{v}} u' \bar{u} dx - \int_a^0 v' \bar{u} dx = \int_a^0 \frac{u'' \bar{u}}{1 - \hat{v}} dx.$$

Integrating the third and fourth terms by parts yields

$$\begin{aligned} & \lambda \int_a^0 \frac{\hat{v}}{1 - \hat{v}} |u|^2 dx + \int_a^0 \left[\frac{\hat{v}}{1 - \hat{v}} + \left(\frac{1}{1 - \hat{v}} \right)' \right] u' \bar{u} dx \\ & \quad + \int_a^0 \frac{|u'|^2}{1 - \hat{v}} dx + \int_a^0 v (\overline{\lambda v + v'}) dx \\ & = \left[v \bar{u} + \frac{u' \bar{u}}{1 - \hat{v}} \right] \Big|_a^0. \end{aligned}$$

Taking the real part, we have

$$(114) \quad \begin{aligned} & \Re e(\lambda) \int_a^0 \left(\frac{\hat{v}}{1 - \hat{v}} |u|^2 + |v|^2 \right) dx + \int_a^0 g(\hat{v}) |u|^2 dx + \int_a^0 \frac{|u'|^2}{1 - \hat{v}} dx \\ & = \Re e \left[v \bar{u} + \frac{u' \bar{u}}{1 - \hat{v}} - \frac{1}{2} \left[\frac{\hat{v}}{1 - \hat{v}} + \left(\frac{1}{1 - \hat{v}} \right)' \right] |u|^2 - \frac{|v|^2}{2} \right] \Big|_a^0, \end{aligned}$$

where

$$g(\hat{v}) = -\frac{1}{2} \left[\left(\frac{\hat{v}}{1 - \hat{v}} \right)' + \left(\frac{1}{1 - \hat{v}} \right)'' \right] \equiv 0$$

and the third term on the right-hand side vanishes, as shown in Section C, leaving

$$\begin{aligned} \Re e(\lambda) \int_a^0 \left(\frac{\hat{v}}{1-\hat{v}} |u|^2 + |v|^2 \right) dx + \int_a^0 \frac{|u'|^2}{1-\hat{v}} dx \\ = \left[\Re e(v\bar{u}) + \frac{\Re e(u'\bar{u})}{1-\hat{v}} - \frac{|v|^2}{2} \right] \Big|_a^0. \end{aligned}$$

A boundary analysis similar to that of Section C shows that the contribution at a on the righthand side vanishes as $a \rightarrow -\infty$; see [12] for details. Thus, in the limit as $a \rightarrow -\infty$ we obtain

$$\begin{aligned} \Re e(\lambda) \int_{-\infty}^0 \left(\frac{\hat{v}}{1-\hat{v}} |u|^2 + |v|^2 \right) dx + \int_{-\infty}^0 \frac{|u'|^2}{1-\hat{v}} dx \\ = \left[\Re e(v\bar{u}) + \frac{\Re e(u'\bar{u})}{1-\hat{v}} - \frac{|v|^2}{2} \right] (0) \\ = \left[(1-v_0) \Re e(v\bar{u}) - \frac{|v|^2}{2} \right] (0), \\ \leq \left[(1-v_0) |v| |u| - \frac{|v|^2}{2} \right] (0) \\ \leq (1-v_0)^2 \frac{|u(0)|^2}{2}, \end{aligned}$$

where the second equality follows by (113) and the final line by Young's inequality.

Next, observe the Sobolev-type bound

$$|u(0)|^2 \leq \left(\int_{-\infty}^0 |u'(x)| dx \right)^2 \leq \int_{-\infty}^0 \frac{|u'|^2}{1-\hat{v}}(x) dx \int_{-\infty}^0 (1-\hat{v})(x) dx,$$

together with

$$\int_{-\infty}^0 (1-\hat{v})(x) dx = \int_{-\infty}^0 -\frac{\hat{v}'}{\hat{v}}(x) dx = \int_{-\infty}^0 (\log \hat{v}^{-1})'(x) dx = \log v_0^{-1},$$

hence $\int_{-\infty}^0 (1-\hat{v})(x) dx < \frac{2}{(1-v_0)^2}$ for $v_0 > v_*$, where $v_* < e^{-2}$ is the unique solution of

$$(115) \quad v_* = e^{-2/(1-v_*)^2}.$$

Thus, for $v_0 > v_*$,

$$(116) \quad \Re e(\lambda) \int_{-\infty}^0 \left(\frac{\hat{v}}{1-\hat{v}} |u|^2 + |v|^2 \right) dx + \epsilon \int_{-\infty}^0 \frac{|u'|^2}{1-\hat{v}} dx \leq 0,$$

for $\epsilon := \frac{(1-v_0)^2}{2} - \frac{1}{\int_{-\infty}^0 (1-\hat{v})(x) dx} > 0$. For $\Re e \lambda \geq 0$, this implies $u' \equiv 0$, or $u \equiv \text{constant}$, which, by $u(-\infty) = 0$, implies $u \equiv 0$. This reduces (110a) to $v' = \lambda v$, yielding the explicit solution $v = C e^{\lambda x}$. By $v(0) = 0$, therefore,

$v \equiv 0$ for $\Re\lambda \geq 0$. It follows that there are no nontrivial solutions of (110), (111) for $\Re\lambda \geq 0$ except at $\lambda = 0$.

By iteration, starting with $v_* \approx 0$, we obtain first $v_* < e^{-2} \approx 0.14$ then $v_* > e^{2/(1-.14)^2} \approx .067$, then $v_* < e^{2/(1-.067)^2} \approx .10$, then $v_* > e^{2/(1-.10)^2} \approx .085$, then $v_* < e^{2/(1-.085)^2} \approx .091$ and $v_* > e^{2/(1-.091)^2} \approx .0889$, terminating with $v_* \approx .0899$. \square

Remark D.1. *Our Evans function results show that the case v_0 small not treated corresponds to the shock limit for which stability is already known by [12]. This suggests that a more sophisticated energy estimate combining the above with a boundary-layer analysis from $x = 0$ back to $x = L + \delta$ might yield nonvanishing for all $1 > v_0 > 0$.*

APPENDIX E. THE CHARACTERISTIC LIMIT: OUTFLOW CASE

We now show stability of compressive outflow boundary layers in the characteristic limit $v_+ \rightarrow 1$, by essentially the same energy estimate used in [18] to show stability of small-amplitude shock waves.

As in the above section on the outflow case, we obtain a system

$$(117a) \quad \lambda \tilde{v} + \tilde{v}' - \tilde{u}' = 0,$$

$$(117b) \quad \lambda \tilde{u} + \tilde{u}' - \frac{h(\hat{v})}{\hat{v}^{\gamma+1}} \tilde{v}' = \frac{\tilde{u}''}{\hat{v}}.$$

identical to that in the integrated shock case [3], but with boundary conditions

$$(118) \quad \tilde{v}'(0) = \frac{\lambda}{\alpha - 1} \tilde{v}(0), \quad \tilde{u}'(0) = \alpha \tilde{v}'(0).$$

In particular,

$$(119) \quad \tilde{u}'(0) = \frac{\lambda\alpha}{\alpha - 1} \tilde{v}(0) = \hat{v}'(0) \tilde{v}(0).$$

This new eigenvalue problem differs spectrally from (22) only at $\lambda = 0$, hence spectral stability of (22) is implied by spectral stability of (117). Hereafter, we drop the tildes, and refer simply to u, v .

Proof of Proposition 3.7. We note that $h(\hat{v}) > 0$. By multiplying (117b) by both the conjugate \bar{u} and $\hat{v}^{\gamma+1}/h(\hat{v})$ and integrating along x from $-\infty$ to 0, we have

$$\int_{-\infty}^0 \frac{\lambda u \bar{u} \hat{v}^{\gamma+1}}{h(\hat{v})} dx + \int_{-\infty}^0 \frac{u' \bar{u} \hat{v}^{\gamma+1}}{h(\hat{v})} dx - \int_{-\infty}^0 v' \bar{u} dx = \int_{-\infty}^0 \frac{u'' \bar{u} \hat{v}^{\gamma}}{h(\hat{v})} dx.$$

Integrating the last three terms by parts and appropriately using (117a) to substitute for u' in the third term gives us

$$\begin{aligned} & \int_{-\infty}^0 \frac{\lambda |u|^2 \hat{v}^{\gamma+1}}{h(\hat{v})} dx + \int_{-\infty}^0 \frac{u' \bar{u} \hat{v}^{\gamma+1}}{h(\hat{v})} dx + \int_{-\infty}^0 v(\overline{\lambda v + v'}) dx + \int_{-\infty}^0 \frac{\hat{v}^\gamma |u'|^2}{h(\hat{v})} dx \\ & = - \int_{-\infty}^0 \left(\frac{\hat{v}^\gamma}{h(\hat{v})} \right)' u' \bar{u} dx + \left[v \bar{u} + \frac{v^\gamma u' \bar{u}}{h(\hat{v})} \right] \Big|_{x=0}. \end{aligned}$$

We take the real part and appropriately integrate by parts to get

$$(120) \quad \Re e(\lambda) \int_{-\infty}^0 \left[\frac{\hat{v}^{\gamma+1}}{h(\hat{v})} |u|^2 + |v|^2 \right] dx + \int_{-\infty}^0 g(\hat{v}) |u|^2 dx + \int_{-\infty}^0 \frac{\hat{v}^\gamma}{h(\hat{v})} |u'|^2 dx = G(0),$$

where

$$g(\hat{v}) = -\frac{1}{2} \left[\left(\frac{\hat{v}^{\gamma+1}}{h(\hat{v})} \right)' + \left(\frac{\hat{v}^\gamma}{h(\hat{v})} \right)'' \right]$$

and

$$G(0) = -\frac{1}{2} \left[\frac{\hat{v}^{\gamma+1}}{h(\hat{v})} + \left(\frac{\hat{v}^\gamma}{h(\hat{v})} \right)' \right] |u|^2 + \Re e \left[v \bar{u} + \frac{v^\gamma u' \bar{u}}{h(\hat{v})} \right] - \frac{|v|^2}{2}$$

evaluated at $x = 0$. Here, the boundary term appearing on the righthand side is the only difference from the corresponding estimate appearing in the treatment of the shock case in [18, 3]. We shall show that as $\hat{v}_+ \rightarrow 1$, the boundary term $G(0)$ is nonpositive. Observe that boundary conditions yield

$$\left[v \bar{u} + \frac{v^\gamma u' \bar{u}}{h(\hat{v})} \right] \Big|_{x=0} = \Re e(v(0) \bar{u}(0)) \left[1 + \frac{\hat{v}^\gamma \hat{v}'}{h(\hat{v})} \right] \Big|_{x=0}.$$

We first note, as established in [18, 3], that $g(\hat{v}) \geq 0$ on $[v_+, 1]$, under certain conditions including the case $\hat{v}_+ \rightarrow 1$. Straightforward computation gives identities:

$$(121) \quad \gamma h(\hat{v}) - \hat{v} h'(\hat{v}) = a\gamma(\gamma - 1) + \hat{v}^{\gamma+1} \quad \text{and}$$

$$(122) \quad \hat{v}^{\gamma-1} \hat{v}_x = a\gamma - h(\hat{v}).$$

Using (121) and (122), we abbreviate a few intermediate steps below:

$$\begin{aligned}
g(\hat{v}) &= -\frac{\hat{v}_x}{2} \left[\frac{(\gamma+1)\hat{v}^\gamma h(\hat{v}) - \hat{v}^{\gamma+1} h'(\hat{v})}{h(\hat{v})^2} + \frac{d}{d\hat{v}} \left[\frac{\gamma\hat{v}^{\gamma-1} h(\hat{v}) - \hat{v}^\gamma h'(\hat{v})}{h(\hat{v})^2} \hat{v}_x \right] \right] \\
&= -\frac{\hat{v}_x}{2} \left[\frac{\hat{v}^\gamma ((\gamma+1)h(\hat{v}) - \hat{v}h'(\hat{v}))}{h(\hat{v})^2} + \frac{d}{d\hat{v}} \left[\frac{\gamma h(\hat{v}) - \hat{v}h'(\hat{v})}{h(\hat{v})^2} (a\gamma - h(\hat{v})) \right] \right] \\
&= -\frac{a\hat{v}_x \hat{v}^{\gamma-1}}{2h(\hat{v})^3} \times \\
&\quad \left[\gamma^2(\gamma+1)\hat{v}^{\gamma+2} - 2(a+1)\gamma(\gamma^2-1)\hat{v}^{\gamma+1} + (a+1)^2\gamma^2(\gamma-1)\hat{v}^\gamma \right. \\
&\quad \left. + a\gamma(\gamma+2)(\gamma^2-1)\hat{v} - a(a+1)\gamma^2(\gamma^2-1) \right]
\end{aligned}$$

(123)

$$\begin{aligned}
&= -\frac{a\hat{v}_x \hat{v}^{\gamma-1}}{2h(\hat{v})^3} \left[(\gamma+1)\hat{v}^{\gamma+2} + \hat{v}^\gamma(\gamma-1)((\gamma+1)\hat{v} - (a+1)\gamma)^2 \right. \\
&\quad \left. + a\gamma(\gamma^2-1)(\gamma+2)\hat{v} - a(a+1)\gamma^2(\gamma^2-1) \right] \\
&\geq -\frac{a\hat{v}_x \hat{v}^{\gamma-1}}{2h(\hat{v})^3} \left[(\gamma+1)\hat{v}^{\gamma+2} + a\gamma(\gamma^2-1)(\gamma+2)\hat{v} - a(a+1)\gamma^2(\gamma^2-1) \right]
\end{aligned}$$

(124)

$$\geq -\frac{\gamma^2 a^3 \hat{v}_x (\gamma+1)}{2h(\hat{v})^3 v_+} \left[\left(\frac{v_+^{\gamma+1}}{a\gamma} \right)^2 + 2(\gamma-1) \left(\frac{v_+^{\gamma+1}}{a\gamma} \right) - (\gamma-1) \right].$$

This verifies $g(\hat{v}) \geq 0$ as $\hat{v}_+ \rightarrow 1$.

Second, examine

$$G(0) = -\frac{1}{2} \left[\frac{\hat{v}^{\gamma+1}}{h(\hat{v})} + \left(\frac{\hat{v}^\gamma}{h(\hat{v})} \right)' \right] |u(0)|^2 + \left[1 + \frac{\hat{v}^\gamma \hat{v}'}{h(\hat{v})} \right] \Re e(v(0)\bar{u}(0)) - \frac{|v(0)|^2}{2}.$$

Applying Young's inequality to the middle term, we easily get

$$G(0) \leq -\frac{1}{2} \left[\frac{\hat{v}^{\gamma+1}}{h(\hat{v})} + \left(\frac{\hat{v}^\gamma}{h(\hat{v})} \right)' - \left(1 + \frac{\hat{v}^\gamma \hat{v}'}{h(\hat{v})} \right)^2 \right] |u(0)|^2 =: -\frac{1}{2} I |u(0)|^2.$$

Now observe that I can be written as

$$I = \frac{\hat{v}^{\gamma+1}}{h(\hat{v})} - 1 + \left[\frac{\gamma\hat{v}^{\gamma-1}}{h(\hat{v})} - \frac{2\hat{v}^\gamma}{h(\hat{v})} - \frac{\hat{v}^{2\gamma}\hat{v}'}{h^2(\hat{v})} \right] \hat{v}' - \frac{\hat{v}^\gamma h'(\hat{v})}{h^2(\hat{v})}.$$

Using (121) and (122), we get

$$\frac{\hat{v}^{\gamma+1}}{h(\hat{v})} - 1 = -\frac{(\gamma-1)\hat{v}^{\gamma-1}\hat{v}' + \hat{v}h'(\hat{v})}{h(\hat{v})}$$

and thus

$$I = -\frac{(\gamma-1)\hat{v}^{\gamma-1}\hat{v}' + \hat{v}h'(\hat{v})}{h(\hat{v})} + \left[\frac{\gamma\hat{v}^{\gamma-1}}{h(\hat{v})} - 2\frac{\hat{v}^\gamma}{h(\hat{v})} - \frac{\hat{v}^{2\gamma}\hat{v}'}{h^2(\hat{v})} \right] \hat{v}' - \frac{\hat{v}^\gamma h'(\hat{v})}{h^2(\hat{v})}.$$

Now since $h'(\hat{v}) = -(\gamma + 1)\hat{v}^\gamma \hat{v}' + (a + 1)\gamma \hat{v}^{\gamma-1} \hat{v}'$, as $\hat{v}_+ \rightarrow 1$, $I \sim -\hat{v}' \geq 0$. Therefore, as \hat{v}_+ is close to 1, $G(0) \leq \frac{1}{4}\hat{v}'(0)|u(0)|^2 \leq 0$. This, $g(\hat{v}) \geq 0$, and (120) give, as \hat{v}_+ is close enough to 1,

$$(125) \quad \Re e(\lambda) \int_{-\infty}^0 \left[\frac{\hat{v}^{\gamma+1}}{h(\hat{v})} |u|^2 + |v|^2 \right] dx + \int_{-\infty}^0 \frac{\hat{v}^\gamma}{h(\hat{v})} |u'|^2 dx \leq 0,$$

which evidently gives stability as claimed. \square

APPENDIX F. NONVANISHING OF D_{in} : EXPANSIVE INFLOW CASE

For completeness, we recall the argument of [19] in the expansive inflow case.

Profile equation. Note that, in the expansive inflow case, we assume $v_0 < v_+$. Therefore we can still follow the scaling (12) to get

$$0 < v_0 < v_+ = 1.$$

Then the stationary boundary layer (\hat{v}, \hat{u}) satisfies (15) with $v_0 < v_+ = 1$. Now by integrating (16) from x to $+\infty$ with noting that $\hat{v}(+\infty) = 1$ and $\hat{v}'(+\infty) = 0$, we get the profile equation

$$\hat{v}' = \hat{v}(\hat{v} - 1 + a(\hat{v}^{-\gamma} - 1)).$$

Note that $\hat{v}' > 0$. We now follow the same method for compressive inflow case to get the following eigenvalue system

$$(126a) \quad \lambda v + v' - u' = 0,$$

$$(126b) \quad \lambda u + u' - (fv)' = \left(\frac{u'}{\hat{v}} \right)'$$

with boundary conditions

$$(127) \quad u(0) = v(0) = 0,$$

where $f(\hat{v}) = \frac{h(\hat{v})}{\hat{v}^{\gamma+1}}$.

Proof of Proposition 3.8. Multiply the equation (126b) by \bar{u} and integrate along x . By integration by parts, we get

$$\lambda \int_0^\infty |u|^2 dx + \int_0^\infty u' \bar{u} + f v \bar{u}' + \frac{|u'|^2}{\hat{v}} dx = 0.$$

Using (126a) and taking the real part of the above yield

$$(128) \quad \Re e \lambda \int_0^\infty |u|^2 + f |v|^2 dx - \frac{1}{2} \int_0^\infty f' |v|^2 dx + \int_0^\infty \frac{|u'|^2}{\hat{v}} dx = 0.$$

Note that

$$f' = \left(1 + a + \frac{a(\gamma^2 - 1)}{\hat{v}^\gamma} \right) \frac{-\hat{v}'}{\hat{v}^2} \leq 0$$

which together with (128) gives $\Re e \lambda < 0$, the proposition is proved. \square

REFERENCES

- [1] J. Alexander, R. Gardner, and C. Jones. A topological invariant arising in the stability analysis of travelling waves. *J. Reine Angew. Math.*, 410:167–212, 1990.
- [2] S. Alinhac. Existence d’ondes de raréfaction pour des systèmes quasi-linéaires hyperboliques multidimensionnels. *Comm. Partial Differential Equations*, 14(2):173–230, 1989.
- [3] B. Barker, J. Humpherys, K. Rudd, and K. Zumbrun. Stability of viscous shocks in isentropic gas dynamics. Preprint, 2007.
- [4] T. J. Bridges, G. Derks, and G. Gottwald. Stability and instability of solitary waves of the fifth-order KdV equation: a numerical framework. *Phys. D*, 172(1-4):190–216, 2002.
- [5] L. Q. Brin and K. Zumbrun. Analytically varying eigenvectors and the stability of viscous shock waves. *Mat. Contemp.*, 22:19–32, 2002. Seventh Workshop on Partial Differential Equations, Part I (Rio de Janeiro, 2001).
- [6] N. Costanzino, K. J. Helge, G. Lyng, and M. Williams. Existence and stability of curved multidimensional detonation fronts. *Indiana Univ. Math. J.*, 56, 2007.
- [7] H. Freistühler and P. Szmolyan. Spectral stability of small shock waves. *Arch. Ration. Mech. Anal.*, 164(4):287–309, 2002.
- [8] R. A. Gardner and K. Zumbrun. The gap lemma and geometric criteria for instability of viscous shock profiles. *Comm. Pure Appl. Math.*, 51(7):797–855, 1998.
- [9] C. M. I. O. Guès, G. Métivier, M. Williams, and K. Zumbrun. Viscous variable-coefficient systems. Preprint, 2006.
- [10] C. M. I. O. Guès, G. Métivier, M. Williams, and K. Zumbrun. Multidimensional stability of small-amplitude noncharacteristic boundary layers. Preprint, 2007.
- [11] O. Guès, G. Métivier, M. Williams, and K. Zumbrun. Existence and stability of multidimensional shock fronts in the vanishing viscosity limit. *Arch. Ration. Mech. Anal.*, 175(2):151–244, 2005.
- [12] J. Humpherys, O. Lafitte, and K. Zumbrun. Stability of isentropic viscous shock profiles in the high-mach number limit. Preprint, 2007.
- [13] J. Humpherys, B. Sandstede, and K. Zumbrun. Efficient computation of analytic bases in Evans function analysis of large systems. *Numer. Math.*, 103(4):631–642, 2006.
- [14] J. Humpherys and K. Zumbrun. A fast algorithm for numerical stability analysis of detonation waves in ZND. In preparation, 2007.
- [15] T. Kato. *Perturbation theory for linear operators*. Classics in Mathematics. Springer-Verlag, Berlin, 1995. Reprint of the 1980 edition.
- [16] S. Kawashima, S. Nishibata, and P. Zhu. Asymptotic stability of the stationary solution to the compressible navier-stokes equations in the half space. *Comm. Math. Phys.*, 240(3):483–500, 2003.
- [17] C. Mascia and K. Zumbrun. Pointwise Green function bounds for shock profiles of systems with real viscosity. *Arch. Ration. Mech. Anal.*, 169(3):177–263, 2003.
- [18] A. Matsumura and K. Nishihara. On the stability of travelling wave solutions of a one-dimensional model system for compressible viscous gas. *Japan J. Appl. Math.*, 2(1):17–25, 1985.
- [19] A. Matsumura and K. Nishihara. Large-time behaviors of solutions to an inflow problem in the half space for a one-dimensional system of compressible viscous gas. *Comm. Math. Phys.*, 222(3):449–474, 2001.
- [20] G. Métivier and K. Zumbrun. Large viscous boundary layers for noncharacteristic nonlinear hyperbolic problems. *Mem. Amer. Math. Soc.*, 175(826):vi+107, 2005.
- [21] R. L. Pego and M. I. Weinstein. Eigenvalues, and instabilities of solitary waves. *Philos. Trans. Roy. Soc. London Ser. A*, 340(1656):47–94, 1992.

- [22] R. Plaza and K. Zumbrun. An Evans function approach to spectral stability of small-amplitude shock profiles. *Discrete Contin. Dyn. Syst.*, 10(4):885–924, 2004. Preprint, 2002.
- [23] F. Rousset. Viscous approximation of strong shocks of systems of conservation laws. *SIAM J. Math. Anal.*, 35(2):492–519 (electronic), 2003.
- [24] H. Schlichting. *Boundary layer theory*. Translated by J. Kestin. 4th ed. McGraw-Hill Series in Mechanical Engineering. McGraw-Hill Book Co., Inc., New York, 1960.
- [25] D. Serre and K. Zumbrun. Boundary layer stability in real vanishing viscosity limit. *Comm. Math. Phys.*, 221(2):267–292, 2001.
- [26] S. Yarahmadian and K. Zumbrun. Pointwise green function bounds and long-time stability of strong noncharacteristic boundary layers. In preparation, 2007.
- [27] K. Zumbrun. Stability of large-amplitude shock waves of compressible Navier-Stokes equations. In *Handbook of mathematical fluid dynamics. Vol. III*, pages 311–533. North-Holland, Amsterdam, 2004. With an appendix by Helge Kristian Jenssen and Gregory Lyng.

DEPARTMENT OF MATHEMATICS, PENNSYLVANIA STATE UNIVERSITY, UNIVERSITY PARK, PA, 16802

E-mail address: `costanzi@math.psu.edu`

DEPARTMENT OF MATHEMATICS, BRIGHAM YOUNG UNIVERSITY, PROVO, UT 84602

E-mail address: `jeffh@math.byu.edu`

DEPARTMENT OF MATHEMATICS, INDIANA UNIVERSITY, BLOOMINGTON, IN 47402

E-mail address: `nguyentt@indiana.edu`

DEPARTMENT OF MATHEMATICS, INDIANA UNIVERSITY, BLOOMINGTON, IN 47402

E-mail address: `kzumbrun@indiana.edu`